

Approaches to spatial confounding in geostatistics

Brian Gilbert¹, Abhirup Datta^{*1}, and Elizabeth L. Ogburn ^{†1}

¹Department of Biostatistics, Johns Hopkins University Bloomberg School of Public Health

January 2022

Abstract

Research in the past few decades has discussed the concept of “spatial confounding” but has provided conflicting definitions and proposed solutions, some of which do not address the issue of confounding as it is understood in the field of causal inference. We give a clear account of spatial confounding as the existence of an unmeasured confounding variable with a spatial structure. Under certain conditions, including the smoothness of the confounder as a function of space, we show that spatial covariates (e.g. latitude and longitude) can be handled as typical covariates by algorithms popular in causal inference. We focus on “double machine learning” (DML) by which flexible models are fit for both the exposure and outcome variables to arrive at a causal estimator with favorable convergence properties. These models avoid restrictive assumptions, such as linearity and heterogeneity, which are present in linear models typically employed in spatial statistics and which can lead to strong bias when violated. We demonstrate the advantages of the DML approach analytically and via extensive simulation studies.

1 Causal inference for spatial data

For most of its history the field of spatial statistics has been concerned primarily with spatial process models, where the goal is prediction and interpolation of a spatially varying outcome Y (e.g. Fuentes (2007), Banerjee et al. (2008), Wikle and Hooten (2010), Stein (2014), Cressie (1993)). However,

^{*}Abhirup Datta was supported by NSF award DMS-1915803.

[†]Elizabeth L. Ogburn and Brian Gilbert were supported by ONR grants N00014-18-1-2760 and N00014-21-1-2820

there is increasing interest in making inferences about the causal effect of an exposure X , possibly also spatially varying, on Y . For the most part, researchers interested in such causal effects have relied on existing spatial models and attempted to clarify when these spatial models can support valid causal inference (Paciorek, 2010; Hodges and Reich, 2010; Schnell and Papadogeorgou, 2020; Keller and Szpiro, 2020). A few papers have drawn from causal inference theory and methods to propose adaptations to existing spatial models (Papadogeorgou et al., 2018; Schnell and Papadogeorgou, 2020; Guan et al., 2020; Osama et al., 2019; Thaden and Kneib, 2018). These papers largely deal with *spatial confounding*: unmeasured variables that are thought to possess a spatial structure and which influence both an exposure and outcome of interest.

We will explore how spatial models relate to the identification assumptions commonly used in causal inference. The motivation for spatial models arises from “Tobler’s First Law of Geography” which states that “everything is related to everything else, but near things are more related than distant things” (Tobler, 1970); spatial models are regression models that take the similarity of spatially proximate observations into account. We will provide a clear statistical framework to understand spatial confounding for geospatial (continuous or point-referenced) data and thoroughly investigate the causal assumptions required for identification of causal effects in its presence. We review existing methods for causal inference in spatial settings and demonstrate conceptually and empirically how some established methods to alleviate spatial confounding fail to address the problem. We then turn to the application of robust methods that have been studied in causal inference but have received little attention in the spatial literature. This includes the method of “double machine learning” (DML) in which flexible models are fit for both outcome and exposure, and the targeting of a “shift estimand,” or the expected change in population-level outcomes if all individuals’ exposures were shifted by a certain amount. We demonstrate that these methods can improve the efficiency, robustness, and interpretability of inference about causal effect in spatial data. As far as we are aware, this is the first approach to spatial confounding that does not rely on restrictive parametric assumptions (such as linearity, effect homogeneity, or Gaussianity) for both identification and estimation.

In Section 2 we review the standard framework for nonparametric identification of causal effects and propose a rigorous definition of “spatial confounding” that is grounded in causal inference. Section 3 reviews existing methods for spatial causal inference and spatial confounding. In Section 4 we unpack the assumptions that will identify causal effects in the presence of spatial confounding

and provide the first fully nonparametric identification results for this setting. We propose shift interventions for spatial causal effects and show how these causal effects are more interpretable and rely on more realistic assumptions than standard causal effects. In Section 5 we demonstrate how flexible machine learning methods can be used in lieu of existing methods for spatial causal inference. These are not limited by parametric assumptions such as effect linearity and homogeneity. These methods are common in the theoretical causal inference literature but we are not aware of them having been used previously in spatial settings. Section 6 is an extensive simulation study demonstrating the fragility of existing methods in the face of violations of parametric assumptions on which they rest and the advantages of DML methods for shift interventions. Section 7 concludes.

2 Spatial and causal confounding

The term “spatial confounding” is frequently used to explain why point estimates from spatial models may be different from point estimates from naive models like ordinary least squares (OLS) that do not use any spatial information. However, this term has rarely been defined explicitly, and we have identified at least four related phenomena that might be referred to as “spatial confounding”:

1. **Omitted variable bias:** The existence of an unmeasured confounding variable with a spatial structure (i.e., an unmeasured variable that obeys Tobler’s law and that influences both the exposure and the outcome) [e.g. Schnell and Papadogeorgou (2020)].
2. **Random effect collinearity:** The change in fixed effect estimates that may come about when spatially-dependent random effects added to a regression model are collinear with the covariates [e.g. Hodges and Reich (2010)].
3. **Regularization bias:** The finite-sample bias of methods that use flexible regression functions like splines or Gaussian processes (GP) to control for an unknown function of space [e.g. Dupont et al. (2020)].
4. **Concurvity:** The difficulty of assessing the effect of an exposure which is, or is close to, a smooth function of space, if an arbitrary smooth function of space is also included in a regression model [discussed in Ramsay et al. (2003); Paciorek (2010)].

The first of these notions of spatial confounding is consistent with standard causal definitions of confounding and is the definition that we will use throughout. The others are statistical notions

that need not be related to causal confounding. Furthermore, as we explain below, random effect collinearity need not be considered a problem, since correctly accounting for confounding should in general entail a change in effect estimates. In the rest of this section we will review causal inference perspectives on confounding and discuss how they apply specifically in spatial settings.

2.1 A brief review of causal inference concepts

Causal effects are typically defined in terms of *potential outcomes* or *counterfactuals*. Let Y be an outcome and X an exposure of interest. A potential or counterfactual outcome $Y(x)$ is the outcome that would have been observed if, possibly contrary to fact, the exposure had been set to value x . Typically only one potential outcome is observed for each unit; the fact that only one of two (if X is binary) or infinite (if X is continuous) potential outcomes can be observed is known as the “fundamental problem of causal inference” (Rubin, 1974). The challenge, then, is to make inferences about the expectation or distribution of potential outcomes despite not being able to fully observe them.

The distribution $\mathcal{P}_{full}(Y(x), X, C)$, where C is the set of measured covariates, is known as the *full data distribution*; it is the joint distribution of covariates, exposure, and the (partially unobserved) potential outcomes. The *observed data distribution* $\mathcal{P}_{obs}(Y, X, C)$ is the joint distribution of covariates, exposure, and the observed outcome. We say that a causal estimand of interest (typically a functional of the full data distribution) is *identified* in a causal model if it can be written as a functional of the observed data distribution.

For the rest of this section we will restrict our attention to the identification of the causal estimand $E[Y(x)]$. If this expectation is identified then so are causal effects such as $E[Y(x)] - E[Y(x')]$, i.e. the expected change in outcomes if X were set to x compared to x' . $E[Y(x)]$ is not identified from the observed data in general, but it can be identified under the following assumptions:

A1 (Consistency). *There are not multiple versions of exposure beyond those recognized by the model: if $X_i = x$, then $Y_i = Y_i(x)$*

A2 (Positivity). *There is positive probability of each exposure at every level of confounders with a positive probability: if $c \in \text{supp}(C)$ and $x \in \text{supp}(x)$, then $(x, c) \in \text{supp}(X, C)$.*

A3 (Conditional ignorability or No unmeasured confounding). *Potential outcomes are independent of exposure assignment conditional on observed confounders: $Y(x) \perp X|C$.*

Confounding is present when ignorability does not hold marginally, that is $Y(x) \not\perp X$. Unmeasured confounding is present if ignorability holds conditional on C, U for some measured confounders C and unmeasured confounders U , but C alone does not suffice for ignorability to hold. That is, there is unmeasured confounding by U if $Y(x) \perp X|C, U$ but $Y(x) \not\perp X|C$. In this paper, we use the term “confounder” to refer to a variable upon which we wish to condition in order to achieve ignorability. (See VanderWeele and Shpitser (2013) for further discussion.)

Under assumptions A1-A3, $E[Y(x)]$ can be identified as follows:

$$\begin{aligned} E[Y(x)] &= E[E[Y(x)|C]] \\ &= E[E[Y(x)|C, X]] \\ &= E[E[Y|C, X = x]] \end{aligned} \tag{1}$$

where the second equality follows from the conditional ignorability assumption, the third from the consistency assumption, and the positivity assumption ensures that the conditioning event has positive probability. The last line is a functional of the observed data alone, known as the *identifying functional*. While these are the typical identifying assumptions in causal inference, other assumptions can also be used to link the full to the observed data distributions. Because these particular identifying assumptions are fully nonparametric, that is they do not place any restrictions on the observed data distribution, we say that $E[Y(x)]$ is *nonparametrically identified*.

Estimation strategies that use the expression in equation (1) to estimate $E[Y(x)]$ rely on a correctly specified outcome regression. An alternative identifying expression allows estimation via *propensity score* (exposure regression) estimation instead:

$$\begin{aligned} E[Y(x)] &= E[E[Y(x)|C]] \\ &= E\left[E\left[Y(x) \frac{I_{X=x}}{P(X=x|C)}|C\right]\right] \\ &= E\left[E\left[Y \frac{I_{X=x}}{P(X=x|C)}|C\right]\right] \\ &= E\left[Y \frac{I_{X=x}}{P(X=x|C)}\right] \end{aligned}$$

where $I_{X=x}$ is the indicator that $X = x$. The first equality holds by the law of iterated expectations, the second by ignorability and positivity (which ensures that the denominator is non-zero), the third by consistency, and the fourth again by iterated expectations. As we will see in Section 5, outcome regression and propensity score regression can be combined to generate *doubly robust* estimation strategies that are consistent for $E[E[Y|C, X = x]] = E\left[Y \frac{I_{X=x}}{P(X=x|C)}\right]$ if either one, but

not necessarily both, of the outcome regression and propensity score models are correctly specified.

2.2 Doubly robust estimation

We return to doubly robust estimation in Section 5. Here we review the basic framework in the context of a binary exposure X .

Let $f(X, C) = E[Y|X, C]$ and $e(C) = P(X = 1|C)$. Assume $\hat{f}(x, c) \rightarrow_{n \rightarrow \infty} \tilde{f}(x, c)$ and $\hat{e}(c) \rightarrow_{n \rightarrow \infty} \tilde{e}(c)$. We *hope* that $\tilde{f} = f$ and $\tilde{e} = e$, but we will explore what happens if only one of the two converges to the truth.

Consider the estimator of $E[Y(1)]$ given by

$$\hat{\mu}_1 = \frac{1}{n} \sum_{i=1}^n \left(\frac{X_i Y_i}{\hat{e}(C_i)} - \frac{X_i - \hat{e}(C_i)}{\hat{e}(C_i)} * \hat{f}(C_i, 1) \right).$$

Under suitable regularity conditions,

$$\hat{\mu}_1 \rightarrow E \left[\frac{XY}{\tilde{e}(C)} - \frac{X - \tilde{e}(C)}{\tilde{e}(C)} * \tilde{f}(C, 1) \right] = E \left[\frac{X * Y(1)}{\tilde{e}(C)} - \frac{X - \tilde{e}(C)}{\tilde{e}(C)} * \tilde{f}(C, 1) \right].$$

Under the identifying assumptions from Section 2.1, this is equal to

$$E[Y(1)] + E \left[\frac{1}{\tilde{e}(C)} * (X - \tilde{e}(C)) * (Y(1) - \tilde{f}(C, 1)) \right].$$

So $\hat{\mu}_1 \rightarrow E[Y(1)]$ if and only if $E \left[\frac{1}{\tilde{e}(C)} * (X - \tilde{e}(C)) * (Y(1) - \tilde{f}(C, 1)) \right] = 0$.

Consider what happens if $\tilde{e} = e$. Then

$$\begin{aligned} & E \left[\frac{1}{\tilde{e}(C)} * (T - \tilde{e}(C)) * (Y(1) - \tilde{f}(C, 1)) \right] \\ &= E \left[E \left[\frac{1}{\tilde{e}(C)} * (X - \tilde{e}(C)) * (Y(1) - \tilde{f}(C, 1)) | Y(1), C \right] \right] \\ &= E \left[E \left[\frac{1}{e(C)} * (X - e(C)) * (Y(1) - \tilde{f}(C, 1)) | Y(1), C \right] \right] \\ &= E \left[\frac{1}{e(C)} * (Y(1) - \tilde{f}(C, 1)) * E[X - e(C) | Y(1), C] \right]. \end{aligned}$$

By ignorability, the inner factor $E[X - e(C) | Y(1), C]$ is equal to $E[X|C] - e(C) = e(C) - e(C) = 0$, and therefore the entire expression is equal to zero, regardless of \tilde{f} .

On the other hand, if $\tilde{f} = f$, then

$$\begin{aligned} & E \left[\frac{1}{\tilde{e}(C)} * (T - \tilde{e}(C)) * (Y(1) - \tilde{f}(C, 1)) \right] \\ &= E \left[E \left[\frac{1}{\tilde{e}(C)} * (X - \tilde{e}(C)) * (Y(1) - \tilde{f}(C, 1)) | C, X \right] \right] \end{aligned}$$

$$\begin{aligned}
&= E \left[E \left[\frac{1}{\tilde{e}(C)} * (X - \tilde{e}(C)) * (Y(1) - f(C, 1)) | C, X \right] \right] \\
&= E \left[\frac{1}{\tilde{e}(C)} * (X - \tilde{e}(C)) * E[(Y(1) - f(C, 1)) | C] \right]
\end{aligned}$$

By ignorability, the inner factor $E[(Y(1) - f(C, 1)) | C, X]$ is equal to $E[Y(1) | C] - f(C, 1) = f(C, 1) - f(C, 1) = 0$. So as before, the estimator is consistent, regardless of \tilde{e} .

A similar argument applies for $E[Y(0)]$. We can consistently estimate expected potential outcomes if *either* $\tilde{f} = f$ or $\tilde{e} = e$. Practically, this means that we only need to correctly specify *either* the outcome model or the propensity score model. Furthermore, the rate of convergence of the doubly robust estimator is typically the *product* of the rates of the convergence of the nuisance estimators, leading to nonparametric *double machine learning* estimators that achieve \sqrt{n} rates (see Chernozhukov et al. 2018) when both the outcome regression and propensity score models are consistently estimated at rate $n^{1/4}$.

2.3 Towards a causally informed definition of spatial confounding

We can now recast the first notion of spatial confounding, omitted variable bias due to a spatially varying unmeasured confounder, in more precise terms. If researchers are interested in estimating the causal effect of a (possibly spatially varying) exposure X on a spatially varying outcome Y , then we will say that there is unmeasured spatial confounding if $Y(x) \not\perp X | C$ but $Y(x) \perp X | C, U$, where C are measured confounders and U is an unmeasured, spatially varying confounder. That is, ignorability does not hold conditional on measured confounders alone but it does hold with the addition of a spatially varying – but unmeasured – confounder U . This unmeasured variable might be a concrete quantity, such as noise pollution levels or household income, but in principle it may be an abstract latent variable.

We emphasize the following fundamental fact: in the presence of arbitrary unmeasured confounding, the identification and estimation of causal effects (i.e., the complete elimination of omitted variable bias) is in general not possible. The presence of an arbitrary unmeasured confounder leaves no imprint on the observed data, and therefore the only approach to control for unmeasured confounding or to mitigate unmeasured confounding bias is to make untestable assumptions that create a bridge between the observed data and the unmeasured confounder. With this fact in mind, the presence of spatial confounding may be seen as a blessing rather than a curse, contrasted with unmeasured

confounding that has no spatial structure. This is because spatial information may be leveraged to capture some of the variability in the confounder and, possibly, to control for some of the confounding. In this case, it is the assumption of a spatial structure that creates the bridge between the observed data and the unmeasured confounder. As we will see below, existing approaches to spatial confounding typically model unmeasured spatial effects with splines or random effects. However, the mere presence of spatial variation in U does not suffice for these spatial methods to mitigate spatial confounding, because whenever an unmeasured confounder has some variation that is *not* spatially determined it is always possible that confounding is due precisely to the non-spatial variation in U . In Section 4 we provide formal conditions under which spatial information suffices to control for unmeasured spatial confounding.

3 Existing approaches to spatial confounding

These methods presented in this section all assume a data generation process where there is residual spatial variation in the outcome beyond what is explained by the covariates and exposure; this variation can be modeled as a fixed or random effect of space. When used for spatial confounding the (sometimes implicit) assumption is that the fixed or random function of space controls for unmeasured spatial confounding. We have identified three assumptions on the data generating process that are commonly made in the existing spatial confounding literature:

1. There exists an unmeasured variable U which is a *fixed* function of spatial location S , and U influences both X and Y . If S is considered random, then U is random as well, and so we may say that U and X are correlated. If S is considered fixed, then U is a nonrandom entity that is empirically associated with X .
2. There exists an unmeasured variable U which is a *random* function of spatial location, and U influences both X and Y . In this case, U is correlated with X whether or not S is random.
3. There exists an unmeasured variable U which is a zero-mean random function of spatial location, and U influences Y , but not X . In this case, U is not a “confounder,” and naive estimators (like OLS) of the effect of X on Y are unbiased, although they may be inefficient or be associated with incorrect standard errors.

It is generally not obvious what scientific contexts justify the consideration of fixed or random effects for the locations in the data generation process. In what follows, we will mainly consider case 1; that is, we assume that there exists an unmeasured variable $U := U(S)$, which is a fixed function of spatial location S and influences both X and Y . If the locations S are considered to be sampled randomly, then $U = U(S)$ is random as well, and so we may say that U and X are correlated. If S is considered fixed, then U is a nonrandom entity that is empirically associated with X . Although in some cases the assumption of random sampling of locations may be unreasonable (e.g. if locations are taken on a regular lattice), the distinction between random and fixed sampling of locations may not be crucial since inference may proceed conditional on the selected locations, assuming they are ancillary to the parameters of interest. With minimal loss of generality we will treat S as random in what follows. Note that the assumption that U is a fixed function of space in the true data generation process should not be confused with the modeling choice to regress Y on a random function of space, e.g. using a Gaussian process regression, which may still be a valid estimation strategy (subject to assumptions) in the same way a fixed parameter can be modeled as a random quantity by assigning a prior in a Bayesian setting.

In spatial statistics literature, it is common to model spatial effects as random functions; we see a few reasons for this. First, physical variables are rarely simple or orderly functions of space, and the complexity of real-world confounding surfaces (that is, a confounding variable as a function of two-dimensional spatial location) may be reminiscent of subjective notions of randomness. And second, Gaussian processes, a particular class of random functions, are popular for their theoretical properties, and they are empirically successful in estimating fixed functions by formally modeling them as random variables. However, there is nothing inherently *random* about the true complex functions or surfaces in most applications. For example, using a Gaussian process to fit topographical elevation does not commit the researcher to any model of how that pattern of elevation came about, and it certainly does not imply that topographical elevation is not a fixed quantity. Deciding whether to model a given variable as stochastic may have more to do with generalization and targets of inference than scientific facts. If we wish to generalize to future iterations of a process that will involve a new confounding surface, then we must have a probabilistic model for this new generation.

We caution that conceiving confounding variables as random functions of space in the true data generation process may lead to spurious claims of estimator unbiasedness. That is, in reality, a confounding variable may exist which leads to estimation error (or *conditional* bias), but in imaginary

re-generations of the confounding variable, the error would average out to zero (an absence of *unconditional* bias). We contend that the latter fact is mostly irrelevant for scientific purposes. We illustrate this with a toy example in Section 3.1.

Conditional on X , measured covariates, and S , we assume that Y is independent and identically distributed (*iid*). Note that this assumption does not ignore spatial dependence; rather it assumes that any spatial dependence is captured by the spatial location of the observations. This is a typical assumption in many spatial regression models that include flexible functions of space in the regression function and assume that residuals are *iid*.

For simplicity we ignore measured confounders C in this section but all of the methods discussed below can immediately accommodate measured covariates. We describe several popular spatial models and approaches to spatial confounding, including recent methods developed explicitly for causal inference. We also include methods for inference about β , the coefficient on X in a regression model of Y on X , because such models are often used in practice to derive evidence about the causal effect of X on Y , even if the models themselves were originally developed for prediction tasks. Finally, note that some methods described below were developed in the context of areal data (spatial data where “location” refers to a region), though we are most interested in geostatistical data, in which locations are point-referenced.

3.1 Ordinary Least Squares

The naive, unadjusted estimate of the effect of X on Y is given by the second component of the ordinary least squares (OLS) estimator

$$\hat{\beta}_{OLS} = (\mathbf{X}'\mathbf{X})^{-1}\mathbf{X}'\mathbf{Y}$$

where the design matrix \mathbf{X} includes the exposure of interest and intercept, and \mathbf{Y} is the vector of outcome values. It is well-known that this procedure does not adjust for spatial confounding, but it is the strawman to which spatial confounding proposals are often compared.

Recall the contention above that conceiving of effects as “random” may lead to spurious claims of estimator unbiasedness. For example, any model can be expanded in such a way as to render the

unadjusted estimator “unbiased.” Consider the following hierarchical model:

$$\begin{aligned} r &\sim \text{unif}(-1, 1) \\ X_i, U_i &\sim_{iid} N\left(\mathbf{0}, \begin{bmatrix} 1 & r \\ r & 1 \end{bmatrix}\right) \\ Y_i &\sim_{iid} N(X_i + U_i, 1) \end{aligned}$$

In any given realization of such a data set, U is a confounding variable and should be included in a regression of Y on X to avoid a (conditionally) biased estimate of the true slope. However, in repeated sampling, the average correlation of U and X is 0, and thus the unadjusted estimator is (unconditionally) unbiased.

3.2 Partially linear models

Many models commonly used to control for spatial effects fall into the class of *partially linear models* (PLM), which may be written

$$Y_i = \alpha + \beta X_i + g(S_i) + \epsilon_i \quad (2)$$

Here, ϵ_i is random error and g is an unknown, smooth function of space. The outcome is linear in the exposure but nonlinear in spatial coordinates, hence the terminology. The estimand β corresponds with the true causal effect of exposure under the assumptions of ignorability and correct specification of the PLM.

Many methods are available to estimate PLMs in spatial contexts. Historically these models were typically used for interpolation (Dubrule, 1984), but more recently researchers have focused on inference about β (e.g. Hodges and Reich (2010), Paciorek (2010), Dupont et al. (2020)). While the PLM often connotes a fixed function g , we note that approaches (described below) such as GP regression, GLS, and random effects models can, under suitable conditions, be consistent for the parameter of a PLM. (Rice, 1986; Yang et al., 2015)

3.2.1 Splines

Splines, or “smoothing splines”, are a family of methods often used to estimate PLMs (equation 2), though PLMs may also be estimated with other methods.

A spline estimator \hat{g} of g is composed of a linear combination of basis functions placed at

various locations (“knots”) in the domain; \hat{g} is constructed so as to minimize in-sample error while maximizing smoothness, typically measured by the “wiggleness” $\int \hat{g}''^2 ds$. (The order of the derivative used to measure wiggleness can vary, but in all following formulas below we will assume order 2.)

As with generalized additive models (GAMs) that have been used to adjust environmental data for time trends (Dominici et al., 2004), certain spline models have become popular for adjusting for spatial trends as captured by g . The model makes no assumption about the relationship between $g(S)$ and X , but in general they may be correlated, in which case $g(S)$ may be interpreted as an unmeasured confounding variable.

Notable for its widespread use is the “thin plate regression spline” (TPRS) (Wood, 2003b), a low-rank smoother which solves certain computational issues associated with approximating functions of multidimensional inputs, S being 2-dimensional for typical spatial applications. Specifically, the spline optimization problem requires a quadratic optimization involving the similarity matrix \mathbf{E} where

$$E_{ij} = \frac{1}{8\pi} r_{ij}^2 \log r_{ij}$$

$$r_{ij} = \|S_i - S_j\|$$

which takes $O(n^3)$ operations, infeasible in large samples. To overcome this, TPRS replaces \mathbf{E} with a rank- k approximation \mathbf{E}_k . With the spectral decomposition

$$\mathbf{E} = \mathbf{U}\mathbf{D}\mathbf{U}'$$

arranged so that the diagonal entries of \mathbf{D} are in descending order of absolute value, we take

$$\mathbf{E}_k = \mathbf{U}_k \mathbf{D}_k \mathbf{U}_k'$$

where \mathbf{U}_k is the first k columns of \mathbf{U} and \mathbf{D}_k is the diagonalization of the first k eigenvalues.

3.2.2 Gaussian process regression

The Gaussian process regression model involves the regression of an outcome variable linearly onto a set of covariates and an additive smooth spatial component $w(S)$, i.e.,

$$Y_i = \alpha + \beta X_i + w(S_i) + \epsilon_i; \quad \epsilon_i \sim N(0, \tau^2) \quad (3)$$

The functional form of GP regression is exactly same as the PLM (equation 2). However, the smooth function w is modeled as a random function and given a Gaussian process (GP) prior. This makes the GP regression model a linear mixed model with a linear covariate fixed effect and a nonlinear spatial random effect modeled as a GP.

A Gaussian process $\mathbf{w} = \{w_l : l \in \lambda\}$, λ being some infinite set, is an infinite collection of random variables such that any finite subset has a multivariate normal distribution. In spatial applications, each variable w_l is associated with a location so that it can be written $w_l = w(S_l)$. This is the point-reference data analog of random effects models for areal data.

For a given domain, the distribution of a Gaussian process is defined by a mean $\mu(s)$ and covariance function $K(S_1, S_2)$. It is common to model Gaussian processes as mean-zero (note that this does not imply that its values in a single realization are centered at zero), isotropic and stationary, which means that $K(S_i, S_j) = K(|S_i - S_j|)$; so a given Gaussian process is determined by a function $K : \mathbb{R} \rightarrow \mathbb{R}$. Throughout, we will consider processes with K in the Matérn family, which is a class of functions widely used in spatial statistics that can be parametrized as

$$K(S_i, S_j | \theta = (\sigma^2, \phi, \nu)) = \frac{\sigma^2}{2^{\nu-1} \Gamma(\nu)} (\phi |S_i - S_j|)^{\nu} \mathcal{K}_{\nu}(\phi |S_i - S_j|); \quad \phi > 0, \nu > 0$$

where Γ denotes the gamma function and \mathcal{K}_{ν} denotes a Bessel function of the second kind (Cressie, 1993).

For estimation in the GP regression model, one can either opt for a fully Bayesian strategy, assigning priors to β and other (covariance) parameters, and proceeding with posterior-based inference. Alternatively, if the errors ϵ_i are *iid* Gaussian with variance τ^2 ; one can marginalize over the spatial random effects w to obtain the marginal likelihood

$$\mathbf{Y} \sim (\beta \mathbf{X}, \mathbf{K}(\theta) + \tau^2 \mathbf{I}) \quad (4)$$

which is then maximized over the parameters β, θ .

Here $\mathbf{K}(\theta)$ is the matrix whose i, j entry is $K(S_i, S_j | \theta)$. τ^2 represents residual noise, which may be referred to as the “nugget” or microvariation.

The maximum marginal likelihood estimate of β is given by the generalized least square (GLS) estimate (see Section 3.3).

3.3 Generalized least squares

A generalized least squares (GLS) model assumes

$$\mathbf{Y} \sim N(\mathbf{X}\beta, \Sigma(\mathbf{s}))$$

where $\Sigma(\mathbf{s})$ is a covariance matrix, typically such that closer pairs of observations have higher correlations than more distant pairs of observations. The relationship between GP and GLS can be seen by recognizing that GLS groups w and ϵ into one correlated error term.

Given Σ , the maximum likelihood estimate for β is

$$\hat{\beta}_{GLS} = (\mathbf{X}'\Sigma^{-1}\mathbf{X})^{-1}\mathbf{X}'\Sigma^{-1}\mathbf{Y}$$

This requires the inversion of the covariance matrix, which can be computationally challenging for large sample sizes.

Note that under the assumption of a multivariate normal distribution for \mathbf{Y} , the expectations of GLS and OLS estimates are identical. The GLS model accounts for dependence in the data, thus improving efficiency and producing valid variance estimators, but does not address bias arising from unmeasured variables. However, GLS estimates coincide (at least theoretically; in practice depending on implementation) with the estimates of marginalized Gaussian process regression, described previously in (4), which is a sensible way of controlling for spatial confounding, in a partially linear model. To understand this, note that the GLS model assumes that errors are uncorrelated with predictors in the data generating process, but the estimation procedure may still be used when this assumption is violated. Therefore, it is possible in theory to use GLS point estimates to control for spatial confounding as long as the model is not taken literally; for example, analytic GLS standard errors should not be used. Furthermore, one should be careful with the implementation of any feasible GLS algorithm (where the correlation parameter is to be estimated from the data), since these algorithms were not designed to control for confounding bias.

3.4 Restricted spatial regression

In the context of areal data, Hodges and Reich (2010) introduced the restricted spatial regression (RSR) model, a version of which we describe here adapted to point-referenced data. RSR is a GP model where it is assumed that the column space of $\mathbf{K}(\theta)$ is orthogonal to X . Beginning with a traditional linear model with random effects

$$\mathbf{Y} = \mathbf{X}\beta + \mathbf{W} + \epsilon \tag{5}$$

with \mathbf{W} capturing spatial effects through a multivariate normal distribution and ϵ being residual noise, we decompose \mathbf{W} using the projection matrix $\mathbf{P}_X = \mathbf{X}(\mathbf{X}'\mathbf{X})^{-1}\mathbf{X}'$ and only use the component orthogonal to \mathbf{X} to give the new model

$$\mathbf{Y} = \mathbf{X}\beta + (\mathbf{I} - \mathbf{P}_X)\mathbf{W} + \epsilon$$

We now have fixed effects and random effects which are completely orthogonal to each other; thus, including the spatial effects does not change the fixed effect estimate and $\hat{\beta}_{RSR} = \hat{\beta}_{OLS}$.

The fact that the traditional mixed-effects model does, like the GP regression model or the GLS estimate, change the fixed effect estimate was seen as a problem by Hodges and Reich (2010), who wrote “it seems perverse to use an error term to adjust for the possibility of missing confounders”; hence the motivation for RSR. This overlooks the fact that such methods can be consistent for the parameter of a PLM, as discussed above. On the other hand, the OLS estimate (and hence the RSR estimate) will certainly be biased in the presence of spatial confounding. As we will demonstrate in Section 4, spatial information can be sufficient to adjust for missing confounders, and the formal mathematical device for doing so, whether it be a spline or a Gaussian process prior, is immaterial as long as the researcher has a clear conception of the goals of the analysis and the assumptions required.

The viewpoint of Hodges and Reich (2010) can perhaps be seen as stemming from assuming the mixed-effects model (equation 5) as the DGP instead of the PLM, in which case we have $E(\mathbf{Y}) = \mathbf{X}\beta$. The GLS estimate, accounting for spatial structure via the error term, will always differ from the OLS estimate in finite samples although both are unbiased estimators. The GLS estimate may also have worse finite sample bias than the OLS one especially if the working covariance matrix of \mathbf{W} is far from the true covariance of \mathbf{W} . However, if (equation 5) is indeed the true DGP, then the OLS will always be unbiased and there is no need for any adjustment like RSR. Indeed, assuming (equation 5) as the true DGP, RSR has been criticized by Khan and Calder (2020) and Zimmerman and Hoef (2021) on the basis of being “anti-conservative” in the context of the linear mixed model (equation 5), but we emphasize that with respect to the issue of causal confounding, RSR does not even attempt to supply an unbiased effect estimate; rather, it assumes there is no confounding bias.

3.5 Spatially-varying coefficient model

A spatially-varying coefficient model (Gelfand et al., 2003) maintains the assumption of a linear outcome regression but allows the slope of the regression to vary by location. The model may be written

$$Y_i = \alpha + g(S) + (\beta + h(S))X_i + \epsilon_i$$

where g, h can either be modeled using spline or Gaussian process and ϵ is an *iid* error term. Here, g controls for confounding and h allows effect heterogeneity, both of which are assumed to be smooth in space. Gelfand et al. (2003) discuss the specification of a Bayesian model, and Gamerman et al.

(2003) evaluate various methods of posterior sampling. Fan and Huang (2005) propose a profile likelihood approach based on frequentist asymptotics. Recent computational advances in profile likelihood model-fitting can be found in Dambon et al. (2021a). Osama et al. (2019) (see Section 3.8.3) make use of a spatially varying coefficient model with improved robustness.

3.6 Two-stage partially linear models

In the spline model, a parameter λ controls the extent of the wiggleness penalty. Higher values of λ penalize wiggleness more; lower values penalize wiggleness less. Under regularity conditions and technical assumptions about the asymptotic regime of the data-generating process, the spline coefficient estimate in the partially linear model has the following properties, assuming $\lambda \approx n^{-\delta}$ for some $0 < \delta < 1$ (Dupont et al., 2020):

$$\begin{aligned} E[\hat{\beta}] - \beta &= o(n^{-1/2}) + O(\lambda^{1/2}) \\ \text{var } \hat{\beta} &= O(n^{-1}) \end{aligned}$$

In order to construct confidence intervals, it is desirable for the bias to converge at a rate faster than the standard deviation. This would require $\lambda = o(n^{-1})$. However, it can be shown that as $n \rightarrow \infty$, the optimal value of λ , as measured by average mean squared error of fitted values (AMSE), satisfies $\lambda = O(n^{-2/3})$, which does not ensure that the bias converges faster than the standard deviation. This is the problem originally identified by Rice (1986); in order to attain suitable convergence rates for coefficient estimates, the spline fit must be “under-smoothed.”

Two methods, the geosadditive structural equation model (gSEM) (Thaden and Kneib, 2018) and spatial+ (Dupont et al., 2020), are designed to alleviate regularization bias in the partially-linear model via two-stage regression; they take the residuals of a spatial spline model of the exposure and use them as explanatory variables in a linear regression of the outcome. (They differ in that the latter includes a spline term in the second regression, while the former does not.)

That is, we first fit the model $X_i = h(S_i) + \delta_i$ and take $\tilde{X}_i = X_i - \hat{h}(S_i)$. Then under gSEM, we write $Y_i = \beta \tilde{X}_i + \epsilon_i$ while for spatial+, we have the model $Y_i = \beta \tilde{X}_i + g(S_i) + \epsilon_i$. Thaden and Kneib (2018) do not give much mathematical analysis of their method, relying mainly on conceptual and simulation-based arguments. As Dupont et al. (2020) write, “it is not immediately clear why the method works.” However, Dupont et al. (2020) give extensive asymptotic results for their own method, spatial+.

Specifically, let λ_x be the penalty parameter of the exposure model and λ be the penalty of the outcome model; assume they satisfy $\lambda \approx n^{-\delta}$, $\lambda_x \approx n^{-\delta_x}$, $0 < \delta, \delta_x < 1$. Letting $\hat{\beta}^+$ denote the new estimator, the following properties hold:

$$E[\hat{\beta}^+] - \beta = o(n^{-1/2}) + O((\lambda\lambda_x)^{1/2})$$

$$\text{var } \hat{\beta}^+ = O(n^{-1})$$

With regularity conditions, however, the AMSE-optimal rates for λ and λ_x are $O(n^{-2/3})$ and $O(n^{-2/3}(\log n)^4)$, respectively. Therefore, with optimal rates, we have $\lambda\lambda_x = o(n^{-1})$, and therefore the bias of the estimate converges faster than the standard deviation, and thus no under-smoothing is necessary.

3.7 Limitations

With the exception of RSR (and OLS, which yields the same estimate), the methods described above can be used to estimate causal effects under two sets of assumptions: (1) causal identification assumptions that ensure that controlling for a flexible function of space suffices to control for unmeasured spatial confounding (see Section 4 for a rigorous exploration of these assumptions), and (2) correct parametric specification of the spatial regression models used in each of these methods. In terms of parametric assumptions, most of the aforementioned methods (except the SVC model) assume homogeneous effects quantified by the coefficient β in the PLM (equation 2) or the LMM (equation 5). Also, all of the methods described above assume linear exposure effects and an additive spatial effect. These assumptions are extremely strong and likely to be unreasonable for many physical exposures. Common toxicological models often include a *threshold*, or a value below which an exposure has negligible effect (Cox, 1987), which is a clear violation of linearity. Recent work in spatial statistics has recognized the shortcoming of the linearity assumption and have extended the Gaussian process regression equation (3) to allow for nonlinear covariate effects fitted flexibly using random forests or boosting thereby creating GLS versions of these machine learning procedures (Saha et al., 2021; Sigrist, 2020). However, these extensions still rely on the additive spatial effect assumption, implying that the effect of exposure is homogeneous in covariates. This may not always be appropriate. For example, in studies of air pollution, linear dose-response models may often be reasonable (Dominici et al., 2002), but air pollution may have more serious effects on the elderly than the young, a violation of homogeneity (Gouveia, 2000).

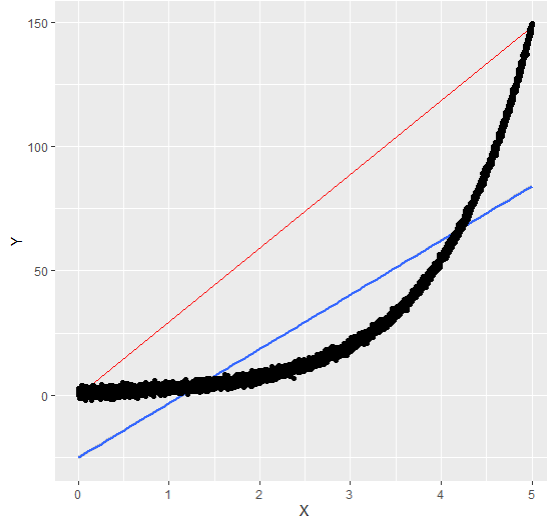


Figure 1: The red line has slope equal to the average incremental effect of intervention on exposure; the blue line is the OLS fit.

Intuitively, researchers may believe that departures from model assumptions of linearity and homogeneity “average out” to yield an accurate estimate even in the presence of model misspecification. Angrist (2003) demonstrates that the average causal effect estimated by a model which (incorrectly) assumes effect homogeneity is an average of the heterogeneous effects weighted by conditional variance of exposure, which may be quite different from the desired uniform average. And if a linear model is used to estimate a nonlinear effect, the resulting estimator need not correspond to a meaningful average, as the following synthetic example demonstrates.

$$X \sim \text{unif}(0, 5), \quad Y \sim N(\exp(X), 1)$$

In this case, the average effect of incremental intervention (that is, the average slope of the dose-response curve) on X may be calculated as

$$E\left[\frac{dE[Y]}{dX}\right] = E[\exp X] = \int_0^5 e^x dx / 5 \approx 29.5$$

But linear regression will approximately minimize $\int_0^5 (e^x - (\beta_0 + \beta_1 x))^2 dx$ which occurs at $(\beta_0, \beta_1) \approx (-24.8, 21.7)$.

This highlights the need for more flexible nonparametric approaches to spatial confounding, and to causal inference in spatial settings more broadly. We propose one such approach in Section 5.

3.8 Recent causal advances

3.8.1 Distance adjusted propensity score matching

For binary exposures $X = 0, 1$, the propensity score $e(C)$ is defined as the probability of receiving exposure conditional on confounders C ; or $e(C) = P(X = 1|C)$. The importance of propensity scores derives from their “balancing property”: if exposure is unconfounded conditional on C , then exposure is unconfounded conditional on $e(C)$. This suggests the procedure of propensity score matching, in which propensity scores are estimated for all individuals, and then treated individuals are matched with untreated individuals with the nearest propensity score. This sample of matched individuals mimics a pseudo-population in which exposure is unconfounded; thus, the effect of exposure in this pseudo-population can be estimated from the observed data. The pseudo-population typically differs from the original population in that it excludes individuals with extreme propensity scores (i.e., those close to zero or one). A review of the use of propensity score matching for confounding adjustment can be found in Stuart (2010).

The traditional propensity score matching procedure is insufficient to control for unmeasured confounding. However, Papadogeorgou et al. (2018) adjust the procedure in a way that may, under causal assumptions like those in Section 4 below, mitigate unmeasured spatial confounding. They introduce a dissimilarity measure d_{ij} where

$$d_{ij} = w * |e(C_i) - e(C_j)| + |S_i - S_j|$$

Thus d_{ij} incorporates relevant differences in observed confounders (as captured through the propensity score) and unobserved confounders (as captured through spatial location), with the weight w determining the relative importance of the two factors. Matching can then proceed based on d_{ij} rather than differences in propensity score alone, which ensures matched individuals are similar based on observed and unobserved confounders.

The advertised strength of this method is that it allows the user to adjust (via w) the relative importance of measured and unmeasured confounders. However, in doing so, the model makes a restrictive assumption about the form of the propensity score, and it is not clear how reliable an *a priori* guess at w could be. On the other hand, if one decides to estimate w from data, it is unclear why this method should be preferred to simply including spatial coordinates in a propensity score model, unless w itself is of substantive interest.

3.8.2 CAR model for areal confounding

The conditionally autoregressive model, originating in Besag (1974), is a computationally convenient correlation model for areal data that encodes the similarity of neighboring areas. If a variable \mathbf{Z} has a mean-zero CAR structure, then

$$\mathbf{Z} \sim N(0, \tau^{-1}(\mathbf{D} - \phi\mathbf{W})^{-1})$$

Here, \mathbf{D} is a diagonal matrix whose entries are the number of neighbors of the corresponding area, and \mathbf{W} is the adjacency matrix of areas. τ and ϕ are free parameters.

Schnell and Papadogeorgou (2020) consider the model

$$Y_i = \eta(X_i, C_i) + g(U_i) + \epsilon_i$$

where C are measured confounders and U are unmeasured confounders. They proceed by letting $g(\mathbf{U}) := \mathbf{U}'$ and assuming $(\mathbf{U}', \mathbf{X})$ has a (joint) CAR structure, thus giving a likelihood model for unmeasured confounding. This differs from a traditional CAR model which only puts the multivariate normal distribution on the random effects, modeling them as independent of the exposure. The paper also considers the estimation of nonlinear effects. However, the method relies on strong parametric identifying assumptions about the relationship between \mathbf{U}' and \mathbf{X} and it is not clear when these would hold in practice or how practitioners would reason clearly about them, especially in settings where U may be an unidentified latent confounder.

3.8.3 Orthogonalized regression for heterogeneous effects

Osama et al. (2019) consider the model

$$Y_i = \beta(S) * X_i + g(S) + \epsilon_i$$

This is equivalent to the spatially-varying coefficient model of Section 3.5, reparametrized for convenience. Taking the residualized versions of the exposure and outcome,

$$W_i := Y_i - E[Y_i|S_i]$$

$$V_i := X_i - E[X_i|S_i]$$

we have the equation

$$W_i = \beta(S_i)V_i + \epsilon_i$$

which eliminates the nuisance function g from the estimation. The authors describe a novel method

for estimating the function β via cubic spline regression in a manner robust to the finite-sample error of the estimates of $E[Y|S]$ and $E[X|S]$. This methodology shares similarities with the spatial+ method of Dupont et al. (2020) (Section 3.6) but has the advantage of handling heterogeneous effects. However, the methodology deals only with linear exposure effects and has not been explored for curve-fitting methods other than splines.

4 Identification and estimability in the presence of spatial confounding

In this section we establish conditions for nonparametric identification of causal effects under spatial confounding using the relevant causal definitions overviewed in Section 2.1. We assume consistency (A1) throughout and, without loss of generality, we omit measured covariates C . We assume the existence of a spatially varying confounder U such that, had U been observed, causal effects of X on Y would be identified. That is, we assume that ignorability and positivity hold conditional on U :

A4. $Y(x) \perp X|U$

and

A5. *If $x \in \text{supp}(X)$ and $u \in \text{supp}(U)$, then $(x, u) \in \text{supp}(X, U)$*

The question we answer in this section is: *Are there assumptions under which causal effects may be estimated using spatial models even if U is unobserved?* In particular, we will present conditions under which spatial location S may be used as a proxy for U . This is the approach taken by all of the methods for spatial confounding considered in the literature – they can be seen as controlling for S in lieu of U . But as we will see, the validity of this approach depends on strong and subtle assumptions. We present one set of sufficient (nonparametric) identification assumptions; other alternatives exist, e.g. the parametric approach of Schnell and Papadogeorgou (2020) for the setting of area-level spatial data, but generally require different analytic methods.

4.1 Ignorability and spatial confounding

Consider draws from a joint distribution \mathcal{P} defined over variables $(S, X, Y(x))$, where S is spatial location, X is some exposure, and $Y(x)$ are potential outcomes. Throughout we make the crucial

and strong assumption that the unmeasured confounder U is spatially varying such that $U = g(S)$, where g is a (possibly unknown) measurable function:

A6. $U = g(S)$ for a fixed, measurable function g .

Note that U may not be unique; that is there may be multiple different random variables that each suffice to control for confounding. Technically, it need only the the case that Assumption A6 holds for some U that satisfies Assumption A4.

There are two ways in which an arbitrary unmeasured confounder could fail to be equal to $g(S)$ for some measurable function g . First, U may not be a function of space; this is the case whenever two individuals may share a location without sharing a value of U . For example, if U is personal income but location is measured at the household level, then U is not a function of S because members of the same household may have different values for personal income.

On the other hand, even if it can be claimed that U is a function of S , it is not necessarily a *measurable* function of S . On a continuous domain, a measurable function can be thought of as a “nearly continuous” function, or a continuous function with at most a small set of discontinuities (see “Lusin’s theorem” in Pugh (2015)). Then even a variable such as household income (as opposed to personal income) does not satisfy this criterion, because the map from spatial location to household income is very discontinuous, as neighboring households may have very different incomes.

In the case that U is a measurable function of space plus some residual variation, as might be assumed for a variable like household income, confounding bias may be reduced but its elimination is in general impossible. In other words, including spatial information in a causal analysis could reduce bias compared to omitting spatial information, but causal estimates would still not be consistent. In this setting, the flexible function of S included in spatial regression models could operate like a surrogate or proxy confounder or a confounder measured with error, but it could not capture the confounder without error. In general, the literature on spatial confounding does not explicitly claim that spatial regression models can eliminate confounding bias; rather the ubiquitous implicit assumption seems to be that a flexible function of S can mitigate bias due to unmeasured spatially varying confounding. But, tempting though it may be to reason that controlling for a mismeasured confounder or a confounder proxy will always mitigate confounding bias, the reality is considerably more complicated (Ogburn and VanderWeele, 2012; Ogburn and Vanderweele, 2013; Kuroki and Pearl, 2014; Lash et al., 2020; Tchetgen et al., 2020; Peña et al., 2021). Following Ogburn and

VanderWeele (2012); Ogburn and Vanderweele (2013), we conjecture that using a flexible function of S to control for an unmeasured spatially varying confounder will tend to mitigate confounding bias whenever the relationship between S and U does not vary with exposure (that is, measurement error is non-differential) *and* there is no qualitative interaction between the unmeasured confounder and the exposure, but future work is needed to prove or further explore this conjecture.

The following proposition characterizes when conditioning on location S in lieu of an unmeasured spatial confounder U suffices for ignorability to hold. First, we make the assumption that conditioning on S in addition to U does not *induce* confounding:

A7. $Y(x) \perp X|S, U$

Proposition 1. *Assumptions A6 and A7 imply $Y(x) \perp X|S$.*

Proof. Since $U = g(S)$ is a measurable function of S , the double (S, U) is a measurable function of S as well. Since S is trivially a function of (S, U) , there exists a measurable one-to-one mapping between S and (S, U) ; therefore S and (S, U) give rise to the same conditional distributions (formally, they generate the same sigma-algebra). Therefore if $Y(x) \perp X|(S, U)$, it also holds that $Y(x) \perp X|S$. \square

Assumption A7 is similar to conditional ignorability A4. If the latter is true, the former is often a reasonable assumption; it would typically hold whenever spatial location is causally precedent to exposure and outcome but would be violated if spatial location were a collider between exposure and outcome (i.e., it is influenced by both exposure and outcome) or a descendant of (i.e., influenced directly or indirectly by) such a collider. The assumption is likely uncontroversial in many applications, though this could be complicated in longitudinal studies, especially if there is movement of subjects. (See Elwert and Winship (2014) for a discussion of collider bias.)

Note that the assumption A7 of the above proposition may be circumvented in favor of the substantively stronger but possibly more intuitive assumption

A8. $(Y(x), X) \perp S|U$

This assumption implies that spatial location only affects the joint distribution of potential outcomes and exposure through the unmeasured confounder. This assumption is reasonable if U is the only (unmeasured) spatial variable affecting X or Y . Together with A4 and A6, this is sufficient for the conclusion of Proposition 1.

4.2 Positivity and spatial confounding

A few sources (Westreich and Cole, 2010; Petersen et al., 2012; D’Amour et al., 2021) have devoted themselves to discussing the details of the positivity assumption (not in the context of spatial confounding), though it receives considerably less attention in the literature than ignorability. In the context of spatial confounding, Paciorek (2010) and Schnell and Papadogeorgou (2020) associated the positivity assumption with the assertion that the exposure varies at a smaller scale than the spatial confounder, a point which is also explored in Keller and Szpiro (2020), but a rigorous treatment of spatial-statistical concepts and the positivity assumption in causal inference is lacking.

As discussed in Section 2, with outcome Y , exposure X , and a measured confounder C , the positivity assumption is needed to ensure that the conditioning event has positive probability in the expression $E[E[Y(x)|C, X = x]]$. If there exists $x \in \text{supp}(X)$ such that $c \in \text{supp}(C)$ and $(x, c) \notin \text{supp}(X, C)$, then the above functional is not well-defined. If positivity fails, then parametric assumptions such as effect linearity or homogeneity are needed to estimate causal effects. These assumptions can be used to extrapolate from regions of the data where positivity holds to regions where it does not hold. We caution that any conclusions drawn from regions of the data where positivity does not hold are not informed by the data; they are determined entirely by the assumptions used to extrapolate.

In the case of spatial confounding, positivity must hold with respect to S in order for inference using S as a proxy for U to avoid extrapolation. In some settings it may be feasible to reason about this directly, i.e. to assume

A9. *If $x \in \text{supp}(X)$ and $S \in \text{supp}(S)$, then $(x, s) \in \text{supp}(X, S)$.*

Alternatively, if researchers do not have enough *a priori* information about the joint distribution of exposure and spacial location to assess whether Assumption A9 is reasonable, positivity with respect to S is also guaranteed by the following assumption in conjunction with A5:

A10. *$X \perp S|U$; that is, S is only associated with X through U .*

The following proposition says that if positivity holds conditional on U , and S is only associated with X through U , then positivity also holds conditional on S :

Proposition 2. *Assume A5 and A10. Then positivity holds conditional on S , meaning if $x \in \text{supp}(X)$ and $s \in \text{supp}(S)$, then $(x, s) \in \text{supp}(X, S)$.*

Proof. By the former assumption, we have $pr(X = x|U) > 0$ for each x . Then, by the latter assumption, $pr(X = x|U, S) > 0$. Since $(U, S) = (g(S), S)$ is a one-to-one function of S , conditioning on (U, S) is equivalent to conditioning on S . Therefore, $pr(X = x|S) > 0$. \square

Note that A10 is implied by A8.

In practice, the relevant consideration regarding positivity conditional on spatial location is whether there is a sufficient mix of exposure levels within reasonably small regions of the confounder space. Alternatively, as discussed in Paciorek (2010), we can interpret positivity as the existence of a finer spatial scale of variation of X compared to U ; if X varies faster than U , then areas with similar values of U will exhibit wide ranges of values of X . For continuous confounders, these interpretations are crucial because the probability associated with any particular confounder value is zero. Note that under the assumption that U is a measurable function of S , then small neighborhoods of S will typically contain small regions of the confounder space U , hence the connection between the two conditions, though we note that a quickly varying function may still be measurable or even continuous (for example, a sinusoidal function with small period) in which case, exposure would need to vary at even higher scale for positivity to hold. Given that in most scientific applications there will be non-infinitesimal space between observations, it may be difficult to differentiate even in principle between a quickly varying smooth function and a non-measurable function, but a thorough discussion of this subtlety is beyond the scope of this paper.

4.3 Estimability

Under assumptions A5, A7, and A10; or A4, A5, and A8; or A7 and A9 (and, in any event assuming A6); causal effects are nonparametrically identified using S instead of U : following the logic of Section 2.1, $E[Y(x)] = E[E[Y|X = x, g(S)]]$. Estimation, however, is complicated by the fact that $g(S)$ is unknown and by the fact that Y could depend on S even after conditioning on $g(S)$. In this section, we discuss two conditions under which a correctly specified outcome regression of Y onto X and S can be used to consistently estimate $E[Y|X = x, g(S)]$ and therefore consistently estimate causal effects under the identifying assumptions above. These conditions are assumed, often implicitly, in the literature reviewed in Section 3, but we caution that they need not hold in general.

First, it must be the case that a single function of space suffices simultaneously to control for

confounding and to control for any additional spatial structure in Y . Otherwise, a regression for $E[Y|X = x, S]$ could capture the dependence in Y due to S at the expense of controlling for confounding. What is at stake here is concurvity: if a function $h(S)$ that captures residual spatial structure in Y after controlling for $g(S)$ is concave with $g(S)$, then in general a regression for $E[Y|X = x, S]$ will fail to fully control for $g(S)$ without strong additional assumptions. Note that assumption 8, which is not required for identification, implies that any spatial structure in Y is due only to U , in which case this would not be a problem. A rigorous discussion of concurvity is beyond the scope of this paper, but we demonstrate it heuristically with the following toy example. Suppose that altitude is an unmeasured confounder of X and Y and is a measurable function of space satisfying the identifying assumptions of Sections 4.1 and 4.2. Although they are not confounders, several other unmeasured spatially varying covariates also affect Y – e.g. access to healthcare, exposure to weather, etc. Taken together, these variables result in spatial structure in Y that can be captured by $h(S)$. Concurvity between $h(S)$ and altitude means that, instead of conditioning on altitude in an outcome regression, we are instead conditioning on an unknown function of altitude and $h(S)$. This is akin to a (non-spatial) setting where age is a confounder but we can only condition on $age + income$. This will fail to fully control for confounding by age except in pathological cases.

Second, it must be the case that the functional form of $E[Y|X = x, S]$ is compatible with the regression surface that matters for confounding, $E[Y|X = x, g(S)]$. Suppose $E[Y|X, U]$ is linear in U but U is a polynomial function of S . Then a linear regression of Y onto X and S would be misspecified but a polynomial regression would be correctly specified. A challenge in the spatial confounding scenario is that the relationship between U and S will generally be an unknown transformation, therefore it may be easier for researchers to reason about modeling assumptions on the basis of U rather than S . This points to the need for flexible nonparametric estimation strategies that have a better chance of capturing the true confounding surface in terms of S .

Conversely, researchers who reason about the functional form of $E[Y|X, S]$ may miss important interaction or other terms needed to capture $E[Y|X, g(S)]$. Suppose the unmeasured confounder U interacts with X in its effect on Y . Then a model for $E[Y|X, S]$ that does not include interactions between X and functions of S cannot hope to control for confounding by U . Again, this highlights the need for flexible nonparametric estimation strategies.

4.4 Shift interventions

So far we have focused on the nonparametric identification of $E[Y(x)]$ – but typically the goal of causal inference is to estimate a causal effect rather than a mean potential outcome. In the simplest case, a binary exposure $X = 0, 1$ admits the notion of an “average treatment effect,” defined as $E[Y(1) - Y(0)]$. When X is continuous, as is often the case with environmental exposures, there is no longer just one quantity which completely specifies the average effect of interventions on X . One might choose to estimate the entire *dose-response curve* $E(Y(x))$ for all values x , but it can be convenient to have a more compact characterization of the effect on of interventions on X . As described in Sec 3, this is typically accomplished by assuming linear and homogeneous treatment effects so that any contrast $E[Y(x) - Y(x')]$ is a simple function of β . However, as we described in Section 3.7, when the operative parametric assumptions do not hold this approach does not necessarily result in interpretable causal effects. While estimation of the dose-response curve has been explored with robust causal methods of the kind we advocate (e.g. Kennedy et al. (2017)), this kind of functional estimation may be difficult and unnecessary if a low-dimensional effect summary is desired. We will provide an alternative approach.

We define a “shift intervention” as a special case of the class of interventions considered in Haneuse and Rotnitzky (2013). A shift intervention is an intervention that assigns to individual i with exposure X_i the new exposure $X_i + \delta$ for some constant δ . Thus the expected effect of the shift intervention on individual i is $E[Y_i(X_i + \delta) - Y_i(X_i)]$; notably, this quantity depends on X_i . If we are interested in population-level effects, we may define $\Delta = E[Y(X + \delta) - Y(X)]$, simply taking the population average of individual effects, where the expectation is taken over the observed data distribution of X . Therefore this expectation depends on the observed data distribution, unlike many causal estimands which depend only on the full data distribution (see Section 2.1). In other words, the effect of the intervention may depend on what values of exposure are already present in the population. For example, in a threshold model, shift interventions in the positive direction might have no effect if current population levels are far below the threshold, but high effects if current population levels are near the threshold.

As noted above, targeting the shift estimand may be beneficial since it avoids estimating entire functions (like the dose-response curve), which is challenging with limited data. Aside from feasibility, the shift estimand is advantageous in that it avoids parametric assumptions and relaxes the requirement

of positivity. The shift estimand is also easily interpretable and of direct policy relevance in many applications.

Specifically, we can replace the positivity assumption A5 or A9 with the following weaker assumption:

$$\mathbf{A11.} \quad (x, c) \in \text{supp}(X, C) \implies (x + \delta, c) \in \text{supp}(X, C)$$

Recall that (standard) positivity would entail that each level of confounder values corresponds to a positive probability of receiving *any* exposure. This assumption, which we may call “shift positivity”, on the other hand, is satisfied if every confounder value has positive probability of exposure values within δ of its observed exposure value. In the case of spatial confounding, if A11 holds for $C = U$, and A10 is satisfied, then A11 also holds for $C = S$; the logic is identical to that of the case of positivity. Shift positivity may be a more reasonable assumption for exposures such as air pollution, where there may be variation over relatively small regions, but not enough variation to cover the entire range of exposure values seen across large regions.

Targeting the shift estimand does not require the assumption of a linear or homogeneous model since it represents the *average* expected change over all subjects if all their exposures were shifted by a certain amount, regardless of whether each subject would be expected to display the same change in outcome. The shift estimand is therefore a way of summarizing causal processes down to one scalar quantity even if the causal process is heterogeneous or nonlinear. (If the shift is infinitesimal, then this corresponds to the discussion of figure 1.) Note that when the true data-generating process is linear in X (i.e., $E[Y|C, X]$ is a linear function of X), the shift intervention estimand for a unit shift coincides with the ordinary linear coefficient, but the coefficient in a linear model signifies the expected change in *every* subject’s outcome that would be brought by a one-unit increase in exposure; for this to be meaningful both linearity and homogeneity must be satisfied.

With this in mind, it is easy to see why the shift estimand is of direct policy relevance: it is more practical to consider interventions that incrementally change each individual’s exposure by some amount (for example, what would be the average effect on life-expectancy if PM2.5 levels were decreased everywhere by $2\mu\text{g}/\text{m}^3$?), rather than adjusting all individuals’ exposure levels to some common new level which may be far from their current values (which is the intervention directly considered by estimation of the dose-response curve). Finally, by summarizing complex data generating processes down to a single quantity, the shift estimand is valuable for its interpretability.

5 Flexible models for spatial confounding

In this section we assume that the identifying assumptions from Section 4 hold, that is that the causal effect of X on Y is nonparametrically identified using S as a proxy to control for unmeasured confounding by U . We now turn to estimation strategies and discuss semi- and nonparametric alternatives to the spatial regression models from Section 3. First we present a general nonparametric spatial regression model, but our focus is on *doubly robust* methods that model both the outcome conditional on X and S , as in the spatial regression methods, and the exposure conditional on S , i.e. the propensity scores. This methodology has been employed in causal inference for decades (see Benkeser et al. (2017) for a relevant exposition) but is rarely employed in spatial statistics. A doubly robust estimator consistently estimates the causal effect of interest if either one of the two models is correctly specified; typically doubly robust estimators are efficient when both are correctly specified. In the case where the outcome and exposure models are both nonparametric, this estimation strategy is referred to as DML. It can be shown that in such models, the asymptotic error of the DML model behaves as a product of the asymptotic errors of the two component models, thus increasing efficiency, improving rates of convergence, and allowing causal effects to be estimated at parametric $n^{1/2}$ rates even when the postulated models only converge at rate $n^{1/4}$ (Chernozhukov et al., 2018).

In general, it is preferable not to impose strong assumptions on the data-generating process, but it is especially important in the context of spatial confounding. This is because any scientific knowledge that could justify restrictive assumptions would likely come from understanding of the process involving the physical unmeasured confounder variable rather than spatial location itself. A more flexible class of regression models than the ones discussed in section 3 may be written as

$$Y_i = f(X, S) + \epsilon_i$$

where S is typically two-dimensional and the error terms ϵ have expectation zero and are independent of confounders, exposure, and each other.

Numerous algorithms may be used to estimate the regression function f . We will use multidimensional spline smooths (in the `mgcv` R package) on the joint space of X and S , multidimensional Gaussian processes (in the `kergp` R package) on the joint space of X and S , random forests (in the `randomForest` R package), and BART (Bayesian additive regression tree, in the `dbarts` R package). The spline and Gaussian processes only rely on the assumption that the regression function is smooth in its

inputs. Tree-based models (random forest and BART) do not make the assumption of a smooth function; rather, they approximate arbitrary functions by estimators that are piecewise constant over rectangles in the input space (Breiman, 2001; Chipman et al., 2010).

Under the identification assumptions, these regression techniques are sufficient to estimate causal parameters including the dose-response curve. However, as mentioned above, it may be difficult and unnecessary to estimate the entire dose-response curve. In addition, as found by Naimi et al. (2020), using machine learning outcome regression alone (as opposed to in a DML framework) to estimate causal parameters with complex confounding can lead to extremely unreliable confidence intervals. By utilizing the shift estimand and doubly-robust methods, we can give more reliable and interpretable results for causal estimands with complex spatial confounding.

5.1 Doubly robust estimation

We now turn to doubly robust estimation, first with parametric outcome and propensity score models and then with DML. Doubly robust versions of the nonparametric outcome regression (equation 5) are available, e.g. Kennedy et al. (2017), but following the discussion in Section 4.4 we instead focus here on methods originally proposed by Haneuse and Rotnitzky (2013) for doubly robust estimation of a shift intervention.

The following provides a discussion of a specific case of the methodology presented in Haneuse and Rotnitzky (2013) to estimate the shift interventions discussed in Section 4.4.

For $\mu_\delta := E[Y(X + \delta)]$ and $E[Y(X)] = \mu_0$, we have $\Delta = \mu_\delta - \mu_0$. The latter term can clearly be estimated by the empirical outcome mean $\hat{\mu} = \bar{y}$, so we will focus on the estimation of the former quantity.

First consider the regression function $f(x, s) = E[Y(X)|X = x, S = s]$. By ignorability, this regression function can be estimated consistently from the observed data, because $E[Y(X)|X = x, S = s] = E[Y|X = x, S = s]$ (see 2.1). With an estimator function \hat{f} , we can consistently estimate μ_δ by $n^{-1} \sum_{i=1}^n \hat{f}(X_i + \delta, S_i) := \hat{\mu}_{\delta, R}$, the outcome regression estimator.

On the other hand, we also have the identity

$$\mu_\delta = E[\lambda(X, S)Y]$$

where

$$\lambda(X, S) = \frac{p(X - \delta|S)}{p(X|S)}$$

with p a probability density, because

$$\begin{aligned} E\lambda(X, S)Y &= \int \int \int \frac{p(X - \delta|S)}{p(X|S)} Y p(S) p(X|S) p(Y|X, S) dS dX dY \\ &= \int \int \int p(X - \delta, S) Y p(Y|X, S) dS dX dY \end{aligned}$$

This is the conditional expectation of Y when X is shifted by δ , and so ignorability yields

$$= E[Y(X + \delta)] = \mu_\delta$$

Thus it is possible to estimate the potential-outcome shifted mean either by modeling the outcome process or the exposure process. In the following way, these two strategies may be combined.

Let \hat{f} be an estimator of $E[Y|X, S]$ and $\hat{\tau}$ be an estimator of $p(X|S)$. We solve the following estimating equation for γ :

$$\sum_{i=1}^n \hat{\lambda}(X_i, S_i) (Y_i - \hat{f}(X_i, S_i) - \gamma \hat{\lambda}(X_i, S_i)) = 0$$

where $\hat{\lambda}$ means an estimate of λ based on $\hat{\tau}$. This equation may be solved by fitting a linear model for Y with the covariate $\hat{\lambda}(X_i, S_i)$, no intercept, and the offset $\hat{f}(X_i, S_i)$. Then the doubly robust estimate of μ_δ is given by

$$\hat{\mu}_{\delta, DR} = n^{-1} \sum_{i=1}^n (\hat{f}(X_i + \delta, S_i) + \gamma \hat{\lambda}(X_i + \delta, S_i))$$

The details of the convergence of $\hat{\mu}_{\delta, DR}$ can be found in the appendix of Haneuse and Rotnitzky (2013). To see the double-robustness, first assume the exposure model is consistent, without any assumption on the outcome regression. Note that for any function h , we have $E[\lambda(X, S)h(X, S)] = E[h(X + \delta, S)]$. Therefore, in large samples, the solution of the estimating equation will converge to the solution of the equation

$$\sum_{i=1}^n \lambda(X_i, S_i) Y_i = \sum_{i=1}^n \hat{f}(X_i + \delta, S_i) + \gamma \lambda(X_i + \delta, S_i)$$

Since $E[\lambda(X_i, S_i) Y_i] = \mu_\delta$, we can divide the above equation by n to see that the law of large numbers implies that $\hat{\mu}_{\delta, DR} \rightarrow \mu_\delta$ as well.

On the other hand, if the outcome regression is consistent, then in large samples, the solution of

the estimating equation will converge to the solution of the equation

$$\begin{aligned}
& \sum_{i=1}^n \hat{\lambda}(X_i, S_i)(Y_i - E[Y_i|X_i, S_i] - \gamma \hat{\lambda}(X_i, S_i)) = 0 \\
& \sum_{i=1}^n \hat{\lambda}(X_i, S_i)(Y_i - E[Y_i|X_i, S_i]) - \gamma \hat{\lambda}^2(X_i, S_i) = 0 \\
& \implies \gamma \rightarrow \frac{\sum_{i=1}^n \hat{\lambda}(X_i, S_i)(Y_i - E[Y_i|X_i, S_i])}{\sum_{i=1}^n \hat{\lambda}^2(X_i, S_i)} \\
& = \frac{n^{-1} \sum_{i=1}^n \hat{\lambda}(X_i, S_i)(Y_i - E[Y_i|X_i, S_i])}{n^{-1} \sum_{i=1}^n \hat{\lambda}^2(X_i, S_i)} \\
& \rightarrow \frac{E[\hat{\lambda}(X_i, S_i)(Y_i - E[Y_i|X_i, S_i])]}{E[\hat{\lambda}^2(X_i, S_i)]}
\end{aligned}$$

Note that $Y - E[X, S]$ is uncorrelated with any function of (X, S) . Therefore, as long as $\hat{\lambda}$ converges some function other than the constant 0, we have $\gamma \rightarrow 0$. Thus $\hat{\mu}_{\delta, DR}$ will asymptotically be based (to the first order) only on \hat{f} and hence consistent. When the outcome regression and exposure models are both consistent $\hat{\mu}_{\delta, DR}$ will achieve the highest possible asymptotic efficiency, as noted by Kennedy (2019).

5.1.1 Double machine learning

Among consistent estimators of an estimand of interest, it is generally preferable to choose one with a fast rate of convergence; in particular, convergence at the rate of $n^{-\frac{1}{2}}$ is desirable for standard asymptotic results and the construction of confidence intervals. When estimating causal effects in the presence of complex or high-dimensional confounding, flexible “machine learning” methods may be beneficial relative to more restrictive methods which risk model misspecification. However, the flexibility of these methods often come at the cost of slower rates of convergence. To combat this difficulty, a strategy similar to doubly robust estimation may be employed via sample-splitting and “orthogonalized” estimation, as laid out in Chernozhukov et al. (2018). A kernel smoothing estimator proposed by Kennedy et al. (2017) specialized this procedure for continuous exposures; the work of Kennedy (2019) offers some general results for interventions that incrementally shift propensity scores.

It can be shown that when machine learning methods are employed to estimate both the outcome and exposure models simultaneously, the exposure effect estimate can converge as quickly as the product of the rates of convergence of those two models, yielding acceptable convergence as long as the models attain the relatively slow rate of $n^{-\frac{1}{4}}$.

Spatial confounding is not necessarily high-dimensional in the sense of involving a high number of adjustment variables, but the complexity of nuisance functions can be expected to be considerable, since any unmeasured confounder may be a complicated function of spatial location, even if that function is smooth. Therefore, the DML is a strong candidate for controlling for spatial confounding.

6 Simulations

The purposes of the following simulations are to show the limitations of restrictive models when their assumptions do not hold, and to compare existing popular estimators with state-of-the-art causal methods, in particular DML. In addition, we simulate scenarios where no methods are capable of returning consistent results due to noise in the confounding surface or smoothness of the exposure. We investigate data-generating processes that involve an unmeasured spatial confounder which influences both exposure and outcome. In each case, the exposure is continuous; the causal contrast of interest is the effect of an intervention shifting the exposure by $(+)$ 1. The locations are generated uniformly at random on the $[-1, 1] \times [-1, 1]$ square, and new locations are drawn in every replicate. In the small-sample simulations, 1000 observations are generated for 500 replicates. In the large-sample simulations, 10,000 observations are simulated for 250 replicates. By design, the true effect in all simulations except the nonlinear effect scenario is 1. In the nonlinear effect scenario, the true effect was assessed by simulation to be 2.431.

6.1 Estimators

The methods under consideration are listed below. Algorithms implemented in external packages are run with default settings. (Due to computational constraints, not every method is used in the large-sample simulations.) Confidence intervals are for 95% nominal coverage. Bootstrap confidence intervals use 120 resamples to obtain a normal approximation to the sampling distribution, as recommended in Efron (1987).

For linear models, we use the linear coefficient estimate to estimate the effect of a $+1$ shift intervention. For other models, other than the DML methods, we use the model to predict potential outcomes under the shift intervention and then take the average difference with the models fitted observed values. For the DML methods, we use the procedure of Haneuse et al. (2019) described above.

- RSR (Hodges and Reich, 2010) (unadjusted estimator). Confidence intervals by bootstrap.
- spline: PLM with spatial effect modeled by thin plate regression spline (Wood, 2003b). Implemented by `mgcv` (Wood, 2003a). Analytic confidence intervals.
- gp: PLM with spatial effect modeled by two-dimensional nearest-neighbors Gaussian process (NNGP) (Saha and Datta, 2018). Implemented by `BRISC` package (Saha and Datta, 2020). Confidence intervals by BRISC bootstrap.
- gSEM: geo-additive structural equation model (Thaden and Kneib, 2018). Splines fit by `mgcv`. Confidence intervals by bootstrap.
- spatial+: `spatial+` (Dupont et al., 2020). Splines fit by `mgcv`. Confidence intervals by bootstrap.
- svc_mle: Spatially-varying coefficient model (Dambon et al., 2021a). Implemented by `varycoef` package (Dambon et al., 2021b). Confidence intervals omitted (since resampled points cannot be accommodated by the GP covariance function).
- spline_interaction: Spline with spatial interaction of exposure and space (hence, a spatially-varying coefficient model). Implemented by `mgcv`. Confidence intervals by bootstrap.
- gp3: Three-dimensional Gaussian process over location and exposure (flexible model). Implemented by `RobustGaSP` (Gu et al., 2020). Confidence intervals omitted (since resampled points cannot be accommodated by the GP covariance function).
- spline3: Three-dimensional spline over location and exposure (flexible model). Implemented by `mgcv`. Confidence intervals omitted due to computational constraints.
- rf: Random forest over location and exposure (flexible model) (Breiman, 2001). Implemented by `randomForest` package (Liaw and Wiener, 2002). Confidence intervals by bootstrap.
- BART: Bayesian additive regression tree (BART) over location and exposure (flexible model) (Chipman et al., 2010). Implemented by `dbarts` (Dorie, 2020) package. Confidence intervals by bootstrap.

- **DML_gp3:** gp3 model augmented with spline model over space for exposure (flexible model, DML). Confidence intervals omitted (since resampled points cannot be accommodated by the GP covariance function).
- **DML_spline:** spline3 model augmented with spline model over space for exposure (flexible model, DML). Confidence intervals omitted due to computational constraints.
- **DML_BART:** BART model augmented with spline model over space for exposure (flexible model, DML). Confidence intervals by bootstrap.

6.2 Notes on implementation

We use package-default settings in general, but we adjust the parameter k in the `mgcv` package which controls the maximum number of degrees of freedom in the spline fits so that they can adequately approximate complicated functions. For splines over two dimensions, we use $k = 200$. For three-dimensional splines, we use $k = 1000$ in the large sample and $k = 500$ in the small sample.

To estimate the effect of the shift intervention by DML, we implement the procedure described in section 5.1. We fit the exposure model with a thin plate regression spline as $X_i = g(S_i) + \epsilon_i$ where the errors are *iid*. The *iid* assumption simplifies the estimation of the function λ (by reducing the conditional density estimation to an unconditional density estimation), but the assumption is violated in the heterogeneous effect simulations (in which case errors are independent but not identically distributed). We introduce heteroskedasticity in these scenarios to demonstrate the potential for bias arising from incorrect assumptions of homogeneity. (Under homoskedasticity, this bias can be zero; see Angrist (2003) which demonstrates that the homogeneous estimate is an average of the population of effects weighted by conditional variance of exposure. Under homoskedasticity, this is equivalent to the unweighted average.)

6.3 Simulation settings and results

We consider the following data-generating processes.

6.3.0 Linear confounding

$$S^a, S^b \sim_{iid} \text{unif}(-1, 1)$$

$$U = S^a + S^b$$

$$X \sim N(U, 5)$$

$$Y \sim N(3U + X, 1)$$

n	method	bias	sd	mse	coverage
1.000×10^3	RSR	7.733×10^{-2}	1.603×10^{-2}	6.237×10^{-3}	0%
1.000×10^3	spline	-9.958×10^{-5}	6.297×10^{-3}	3.958×10^{-5}	96%
1.000×10^3	gp	7.932×10^{-4}	6.509×10^{-3}	4.292×10^{-5}	95%
1.000×10^3	gSEM	1.362×10^{-3}	7.017×10^{-3}	5.099×10^{-5}	99%
1.000×10^3	spatial+	5.348×10^{-4}	6.477×10^{-3}	4.216×10^{-5}	98%
1.000×10^3	svc_mle	3.294×10^{-4}	6.434×10^{-3}	4.143×10^{-5}	
1.000×10^3	spline_interaction	-9.566×10^{-5}	6.338×10^{-3}	4.010×10^{-5}	99%
1.000×10^3	gp3	-5.282×10^{-4}	6.478×10^{-3}	4.216×10^{-5}	
1.000×10^3	spline3	1.538×10^{-5}	6.539×10^{-3}	4.268×10^{-5}	
1.000×10^3	rf	-1.886×10^{-1}	1.370×10^{-2}	3.575×10^{-2}	0%
1.000×10^3	BART	-2.754×10^{-3}	1.340×10^{-2}	1.868×10^{-4}	100%
1.000×10^3	DML_gp3	-2.531×10^{-4}	6.690×10^{-3}	4.473×10^{-5}	
1.000×10^3	DML_spline	1.424×10^{-4}	6.749×10^{-3}	4.548×10^{-5}	
1.000×10^3	DML_BART	-1.811×10^{-3}	1.350×10^{-2}	1.850×10^{-4}	100%
1.000×10^4	RSR	7.715×10^{-2}	5.237×10^{-3}	5.980×10^{-3}	0%
1.000×10^4	spline	-2.203×10^{-4}	1.914×10^{-3}	3.696×10^{-6}	96%
1.000×10^4	gp	-1.842×10^{-4}	1.978×10^{-3}	3.932×10^{-6}	96%
1.000×10^4	gSEM	3.427×10^{-6}	1.934×10^{-3}	3.724×10^{-6}	98%
1.000×10^4	spatial+	-1.298×10^{-4}	1.912×10^{-3}	3.657×10^{-6}	97%
1.000×10^4	spline_interaction	-2.171×10^{-4}	1.911×10^{-3}	3.684×10^{-6}	97%
1.000×10^4	spline3	-1.965×10^{-4}	1.935×10^{-3}	3.768×10^{-6}	
1.000×10^4	rf	-9.426×10^{-2}	4.410×10^{-3}	8.904×10^{-3}	0%
1.000×10^4	BART	-8.981×10^{-4}	2.987×10^{-3}	9.694×10^{-6}	98%
1.000×10^4	DML_spline	-1.965×10^{-4}	1.991×10^{-3}	3.987×10^{-6}	
1.000×10^4	DML_BART	-3.668×10^{-4}	2.992×10^{-3}	9.053×10^{-6}	98%

Table 0: Simulation results in the linear confounding scenario

The linear confounding scenario, Table 0, is a baseline scenario where there is no complicated spatial confounding; the spatial coordinates enter the data generating process linearly. Therefore, all models except for RSR are correctly specified, and regularization bias for spline models is not a concern (since oversmoothing is not possible). All models that adjust for confounding perform well and have high confidence interval coverage except for random forest. We will see the random forest performs poorly in most scenarios, apparently due to inappropriate flattening of estimated outcomes at the extremes of exposure values. While random forest is typically a good prediction

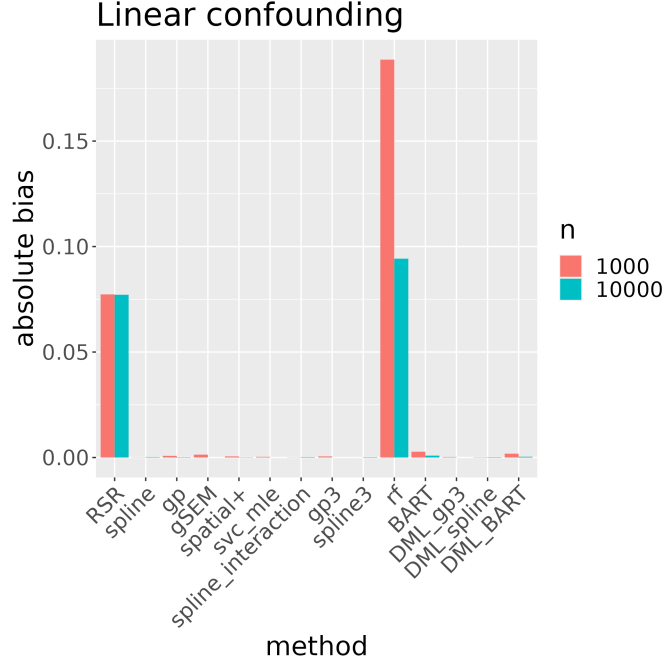


Figure 0: Absolute bias in the linear confounding scenario

algorithm, we caution against off-the-shelf use for counterfactual inference (Wager and Athey, 2018; Lei and Candès, 2021).

6.3.1 Simple effect

$$S^a, S^b \sim_{iid} \text{unif}(-1, 1)$$

$$U = \sin(2\pi S^a * S^b) + S^a + S^b$$

$$X \sim N(U^3, 5)$$

$$Y \sim N(3U + X, 1)$$

In the simple effect scenario, Table 1, the confounding surface is smooth, and the effect is linear and homogeneous, so all models other than RSR are correctly specified. For this reason, almost all models exhibit relatively low error, although random forest performs poorly. However, the flexible models in general perform competitively even with the simpler models, especially gp3 and DML_gp3. The spatial+ algorithm, as advertised, improves on the confidence interval coverage of the spline method in the large sample, but the gSEM confidence intervals fail. The gp method suffers from undercoverage, but note that the BRISC bootstrap confidence intervals are designed for random

n	method	bias	sd	mse	coverage
1.000×10^3	RSR	2.589×10^{-1}	1.528×10^{-2}	6.727×10^{-2}	0%
1.000×10^3	spline	6.863×10^{-3}	6.502×10^{-3}	8.930×10^{-5}	81%
1.000×10^3	gp	7.727×10^{-3}	6.770×10^{-3}	1.054×10^{-4}	76%
1.000×10^3	gSEM	7.305×10^{-2}	7.584×10^{-3}	5.394×10^{-3}	0%
1.000×10^3	spatial+	1.084×10^{-2}	6.826×10^{-3}	1.641×10^{-4}	73%
1.000×10^3	svc_mle	7.387×10^{-3}	6.855×10^{-3}	1.015×10^{-4}	
1.000×10^3	spline_interaction	6.801×10^{-3}	6.568×10^{-3}	8.930×10^{-5}	96%
1.000×10^3	gp3	2.682×10^{-3}	6.939×10^{-3}	5.524×10^{-5}	
1.000×10^3	spline3	6.308×10^{-2}	4.068×10^{-2}	5.631×10^{-3}	
1.000×10^3	rf	-1.458×10^{-1}	1.595×10^{-2}	2.152×10^{-2}	0%
1.000×10^3	BART	7.672×10^{-3}	1.680×10^{-2}	3.405×10^{-4}	100%
1.000×10^3	DML_gp3	1.396×10^{-3}	7.065×10^{-3}	5.177×10^{-5}	
1.000×10^3	DML_spline	2.998×10^{-2}	3.476×10^{-2}	2.104×10^{-3}	
1.000×10^3	DML_BART	3.432×10^{-3}	1.685×10^{-2}	2.950×10^{-4}	100%
1.000×10^4	RSR	2.580×10^{-1}	4.749×10^{-3}	6.661×10^{-2}	0%
1.000×10^4	spline	1.630×10^{-3}	1.947×10^{-3}	6.433×10^{-6}	86%
1.000×10^4	gp	2.159×10^{-3}	1.990×10^{-3}	8.605×10^{-6}	81%
1.000×10^4	gSEM	1.564×10^{-2}	2.089×10^{-3}	2.488×10^{-4}	0%
1.000×10^4	spatial+	5.063×10^{-4}	1.958×10^{-3}	4.075×10^{-6}	96%
1.000×10^4	spline_interaction	1.614×10^{-3}	1.945×10^{-3}	6.372×10^{-6}	88%
1.000×10^4	spline3	2.244×10^{-2}	6.780×10^{-3}	5.495×10^{-4}	
1.000×10^4	rf	-7.677×10^{-2}	4.497×10^{-3}	5.914×10^{-3}	0%
1.000×10^4	BART	2.642×10^{-3}	3.618×10^{-3}	2.002×10^{-5}	97%
1.000×10^4	DML_spline	6.870×10^{-3}	7.080×10^{-3}	9.712×10^{-5}	
1.000×10^4	DML_BART	4.626×10^{-4}	3.586×10^{-3}	1.302×10^{-5}	100%

Table 1: Simulation results in the simple effect scenario

functions rather than the fixed confounding surfaces used here. Use of DML improves on the bias of each machine learning algorithm.

6.3.2 Spatially structured heterogeneous effect

$$S^a, S^b \sim_{iid} \text{unif}(-1, 1)$$

$$U = \sin(2\pi S^a * S^b) + S^a + S^b$$

$$X \sim N(U^3, 5 * \exp(U/2))$$

$$Y \sim N(3U + (1 + U) * X, 1)$$

In the structural heterogeneous effect scenario, 2, only the flexible models, svc_mle, and spline_interaction are correctly specified. The exposure model of the DML models are misspecified in the variance structure, but correctly specified in the mean structure. This heterogeneity, since it is driven by the confounding variable, does cause severe bias in all methods that assume a constant effect. Most

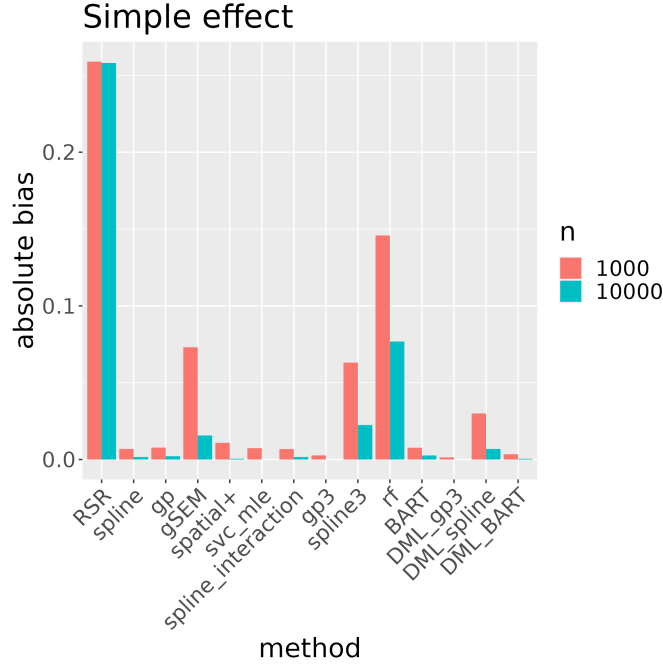


Figure 1: Absolute bias in the simple effect scenario

methods, except for spline_interaction, suffer from undercoverage. Although the DML models do not have full nominal coverage (possibly due to the misspecification of the exposure model), they still show some benefit over their corresponding non-DML methods in terms of bias and MSE. In the small sample, gp3 and DML_gp3 have the lowest MSE; lower even than the simpler methods svc_mle and spline_interaction. The gp3 models are unavailable in the large sample regime, in which spline_interaction has the lowest bias and MSE. Use of DML improves on the bias of each machine learning algorithm.

6.3.3 Nonlinear effect

$$S^a, S^b \sim_{iid} \text{unif}(-1, 1)$$

$$U = \sin(2\pi S^a * S^b) + S^a + S^b$$

$$X \sim N(U^3, 5)$$

$$Y \sim N(3U + X + X^2, 1)$$

Only the flexible models are correctly specified in the nonlinear effect scenario, Table 3; all other methods exhibit substantial bias. Only the BART methods have good confidence interval coverage.

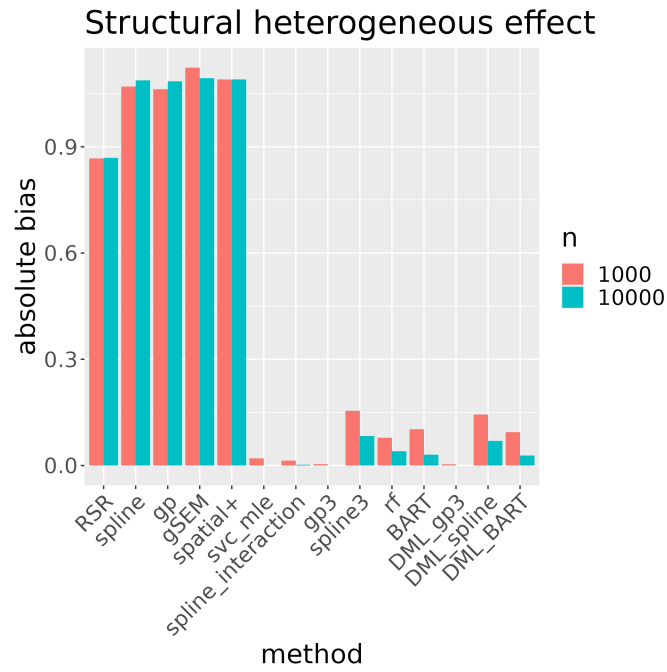


Figure 2: Absolute bias in the spatially-structured heterogeneous effect scenario

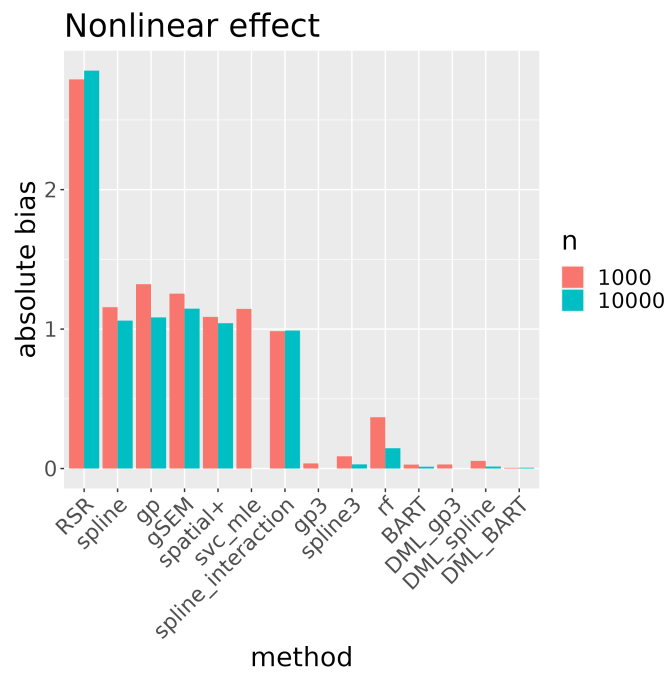


Figure 3: Absolute bias in the nonlinear effect scenario

n	method	bias	sd	mse	coverage
1.000×10^3	RSR	8.670×10^{-1}	1.173×10^{-1}	7.655×10^{-1}	0%
1.000×10^3	spline	1.070×10^0	7.224×10^{-2}	1.150×10^0	0%
1.000×10^3	gp	1.063×10^0	7.418×10^{-2}	1.135×10^0	0%
1.000×10^3	gSEM	1.123×10^0	7.587×10^{-2}	1.268×10^0	0%
1.000×10^3	spatial+	1.090×10^0	7.215×10^{-2}	1.193×10^0	0%
1.000×10^3	svc_mle	2.019×10^{-2}	3.384×10^{-2}	1.551×10^{-3}	
1.000×10^3	spline_interaction	1.390×10^{-2}	3.400×10^{-2}	1.347×10^{-3}	94%
1.000×10^3	gp3	3.863×10^{-3}	3.541×10^{-2}	1.266×10^{-3}	
1.000×10^3	spline3	1.545×10^{-1}	1.074×10^{-1}	3.539×10^{-2}	
1.000×10^3	rf	-7.837×10^{-2}	4.106×10^{-2}	7.824×10^{-3}	67%
1.000×10^3	BART	1.024×10^{-1}	7.197×10^{-2}	1.566×10^{-2}	90%
1.000×10^3	DML_gp3	3.363×10^{-3}	3.541×10^{-2}	1.262×10^{-3}	
1.000×10^3	DML_spline	1.439×10^{-1}	1.073×10^{-1}	3.220×10^{-2}	
1.000×10^3	DML_BART	9.417×10^{-2}	7.194×10^{-2}	1.403×10^{-2}	92%
1.000×10^4	RSR	8.687×10^{-1}	4.060×10^{-2}	7.562×10^{-1}	0%
1.000×10^4	spline	1.088×10^0	2.393×10^{-2}	1.183×10^0	0%
1.000×10^4	gp	1.085×10^0	2.416×10^{-2}	1.178×10^0	0%
1.000×10^4	gSEM	1.094×10^0	2.423×10^{-2}	1.197×10^0	0%
1.000×10^4	spatial+	1.090×10^0	2.389×10^{-2}	1.189×10^0	0%
1.000×10^4	spline_interaction	2.216×10^{-3}	1.080×10^{-2}	1.210×10^{-4}	94%
1.000×10^4	spline3	8.317×10^{-2}	2.091×10^{-2}	7.353×10^{-3}	
1.000×10^4	rf	-4.038×10^{-2}	1.200×10^{-2}	1.774×10^{-3}	16%
1.000×10^4	BART	3.066×10^{-2}	1.514×10^{-2}	1.168×10^{-3}	67%
1.000×10^4	DML_spline	6.955×10^{-2}	2.175×10^{-2}	5.308×10^{-3}	
1.000×10^4	DML_BART	2.832×10^{-2}	1.504×10^{-2}	1.027×10^{-3}	74%

Table 2: Spatially-structured heterogeneous effect simulation results

For both sample sizes, DML_BART has the lowest bias, and use of DML improves on the bias of each machine learning algorithm.

6.3.4 Random heterogeneous effect

$$S^a, S^b \sim_{iid} \text{unif}(-1, 1)$$

$$U = \sin(2\pi S^a * S^b) + S^a + S^b$$

$$X \sim N(U^3, 5 * \exp(U/2))$$

$$d \sim N(0, 1)$$

$$Y \sim N(U + (1 + d) * X, 1)$$

In the random heterogeneous effect scenario, Table 4, no model is correctly specified since the effect varies in a way that is not a well-behaved function of space. However, the randomness in the heterogeneity avoids most estimation bias; it is rather the variance of the methods that are increased

n	method	bias	sd	mse	coverage
1.000×10^3	RSR	-2.791×10^0	1.065×10^0	8.921×10^0	0%
1.000×10^3	spline	-1.157×10^0	6.826×10^{-1}	1.804×10^0	25%
1.000×10^3	gp	-1.322×10^0	6.891×10^{-1}	2.221×10^0	17%
1.000×10^3	gSEM	-1.254×10^0	7.258×10^{-1}	2.098×10^0	55%
1.000×10^3	spatial+	-1.087×10^0	6.927×10^{-1}	1.661×10^0	63%
1.000×10^3	svc_mle	-1.145×10^0	2.002×10^{-1}	1.350×10^0	
1.000×10^3	spline_interaction	-9.852×10^{-1}	4.471×10^{-1}	1.170×10^0	38%
1.000×10^3	gp3	3.652×10^{-2}	3.773×10^{-1}	1.434×10^{-1}	
1.000×10^3	spline3	8.767×10^{-2}	3.791×10^{-1}	1.511×10^{-1}	
1.000×10^3	rf	-3.678×10^{-1}	3.409×10^{-1}	2.513×10^{-1}	75%
1.000×10^3	BART	2.818×10^{-2}	3.902×10^{-1}	1.527×10^{-1}	98%
1.000×10^3	DML_gp3	2.911×10^{-2}	3.771×10^{-1}	1.428×10^{-1}	
1.000×10^3	DML_spline	5.456×10^{-2}	3.765×10^{-1}	1.444×10^{-1}	
1.000×10^3	DML_BART	4.759×10^{-3}	3.901×10^{-1}	1.519×10^{-1}	98%
1.000×10^4	RSR	-2.853×10^0	3.774×10^{-1}	8.283×10^0	0%
1.000×10^4	spline	-1.061×10^0	2.014×10^{-1}	1.166×10^0	0%
1.000×10^4	gp	-1.084×10^0	2.010×10^{-1}	1.215×10^0	0%
1.000×10^4	gSEM	-1.146×10^0	2.053×10^{-1}	1.356×10^0	0%
1.000×10^4	spatial+	-1.042×10^0	2.014×10^{-1}	1.126×10^0	0%
1.000×10^4	spline_interaction	-9.893×10^{-1}	1.594×10^{-1}	1.004×10^0	0%
1.000×10^4	spline3	2.979×10^{-2}	1.229×10^{-1}	1.594×10^{-2}	
1.000×10^4	rf	-1.456×10^{-1}	1.143×10^{-1}	3.421×10^{-2}	75%
1.000×10^4	BART	1.308×10^{-2}	1.253×10^{-1}	1.581×10^{-2}	96%
1.000×10^4	DML_spline	1.421×10^{-2}	1.229×10^{-1}	1.524×10^{-2}	
1.000×10^4	DML_BART	5.706×10^{-3}	1.254×10^{-1}	1.569×10^{-2}	96%

Table 3: Nonlinear effect simulation results

relative to the simple effect scenario. The DML_BART method has the lowest bias for each sample size, while spatially-varying coefficient models have the lowest MSE. Use of DML improves on the bias of each machine learning algorithm.

6.3.5 Noisy confounding

$$S^a, S^b \sim_{iid} \text{unif}(-1, 1)$$

$$U \sim N(\sin(2\pi S^a * S^b) + S^a + S^b, 1)$$

$$X \sim N(U^3, 5)$$

$$Y \sim N(5U + X, 1)$$

In the noisy confounding scenario, Table 5, no method is capable of controlling for the confounding surface because it is not a measurable function of spatial location. All models exhibit substantial error.

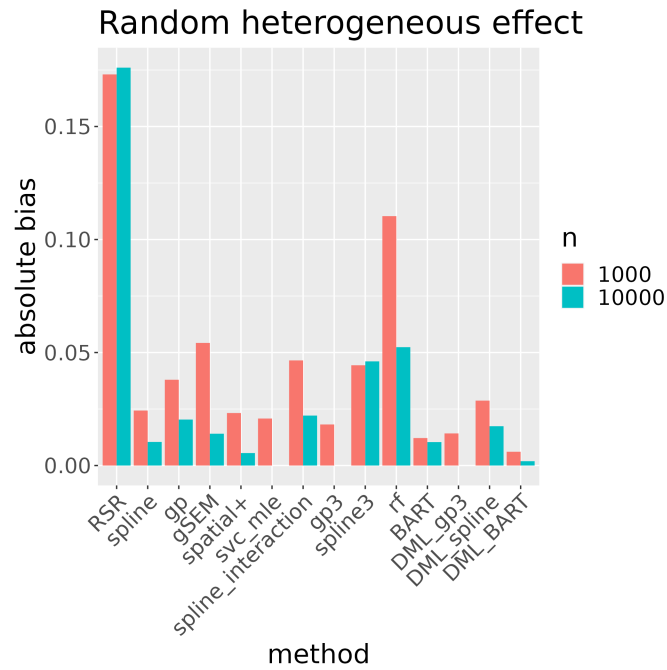


Figure 4: Absolute bias in the random heterogeneous effect scenario

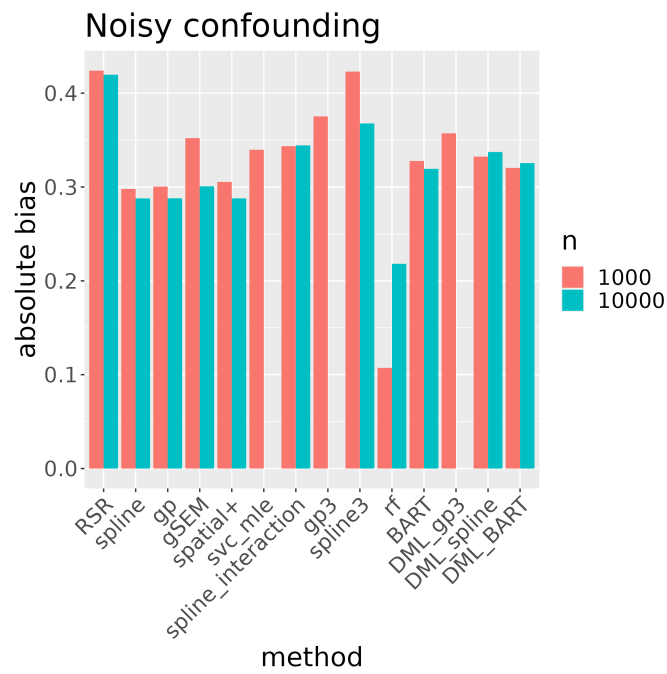


Figure 5: Absolute bias in the noisy confounding scenario

n	method	bias	sd	mse	coverage
1.000×10^3	RSR	1.731×10^{-1}	8.450×10^{-2}	3.707×10^{-2}	0%
1.000×10^3	spline	2.433×10^{-2}	8.790×10^{-2}	8.302×10^{-3}	51%
1.000×10^3	gp	3.795×10^{-2}	8.729×10^{-2}	9.044×10^{-3}	51%
1.000×10^3	gSEM	5.425×10^{-2}	9.213×10^{-2}	1.141×10^{-2}	90%
1.000×10^3	spatial+	2.323×10^{-2}	9.081×10^{-2}	8.770×10^{-3}	93%
1.000×10^3	svc_mle	2.079×10^{-2}	3.639×10^{-2}	1.754×10^{-3}	
1.000×10^3	spline_interaction	4.651×10^{-2}	5.233×10^{-2}	4.896×10^{-3}	94%
1.000×10^3	gp3	1.817×10^{-2}	1.390×10^{-1}	1.962×10^{-2}	
1.000×10^3	spline3	4.436×10^{-2}	2.268×10^{-1}	5.331×10^{-2}	
1.000×10^3	rf	-1.103×10^{-1}	5.951×10^{-2}	1.571×10^{-2}	72%
1.000×10^3	BART	1.216×10^{-2}	1.014×10^{-1}	1.040×10^{-2}	100%
1.000×10^3	DML_gp3	-1.420×10^{-2}	1.363×10^{-1}	1.874×10^{-2}	
1.000×10^3	DML_spline	2.872×10^{-2}	2.301×10^{-1}	5.369×10^{-2}	
1.000×10^3	DML_BART	6.093×10^{-3}	1.023×10^{-1}	1.048×10^{-2}	100%
1.000×10^4	RSR	1.760×10^{-1}	2.928×10^{-2}	3.184×10^{-2}	0%
1.000×10^4	spline	1.043×10^{-2}	2.919×10^{-2}	9.573×10^{-4}	52%
1.000×10^4	gp	2.034×10^{-2}	2.946×10^{-2}	1.278×10^{-3}	47%
1.000×10^4	gSEM	1.407×10^{-2}	2.939×10^{-2}	1.058×10^{-3}	90%
1.000×10^4	spatial+	5.516×10^{-3}	2.923×10^{-2}	8.816×10^{-4}	93%
1.000×10^4	spline_interaction	2.210×10^{-2}	1.800×10^{-2}	8.110×10^{-4}	80%
1.000×10^4	spline3	4.608×10^{-2}	2.875×10^{-2}	2.947×10^{-3}	
1.000×10^4	rf	-5.237×10^{-2}	2.216×10^{-2}	3.231×10^{-3}	62%
1.000×10^4	BART	1.036×10^{-2}	3.330×10^{-2}	1.212×10^{-3}	100%
1.000×10^4	DML_spline	1.740×10^{-2}	3.327×10^{-2}	1.405×10^{-3}	
1.000×10^4	DML_BART	1.913×10^{-3}	3.456×10^{-2}	1.193×10^{-3}	100%

Table 4: Random heterogeneous effect simulation results

6.3.6 Less noisy confounding

$$S^a, S^b \sim_{iid} \text{unif}(-1, 1)$$

$$U \sim N(\sin(2\pi S^a * S^b) + S^a + S^b, 0.1)$$

$$X \sim N(U^3, 5)$$

$$Y \sim N(5U + X, 1)$$

In the less noisy confounding scenario, Table 6, all models are still misspecified, though the smaller departure from smooth confounding allows reasonable estimates, with results more similar to the simple effect scenario.

n	method	bias	sd	mse	coverage
1.000×10^3	RSR	4.240×10^{-1}	3.038×10^{-2}	1.807×10^{-1}	0%
1.000×10^3	spline	2.979×10^{-1}	2.432×10^{-2}	8.936×10^{-2}	0%
1.000×10^3	gp	3.004×10^{-1}	2.442×10^{-2}	9.086×10^{-2}	0%
1.000×10^3	gSEM	3.521×10^{-1}	2.521×10^{-2}	1.246×10^{-1}	0%
1.000×10^3	spatial+	3.055×10^{-1}	2.443×10^{-2}	9.391×10^{-2}	0%
1.000×10^3	svc_mle	3.397×10^{-1}	2.318×10^{-2}	1.160×10^{-1}	
1.000×10^3	spline_interaction	3.436×10^{-1}	1.890×10^{-2}	1.184×10^{-1}	0%
1.000×10^3	gp3	3.753×10^{-1}	2.096×10^{-2}	1.413×10^{-1}	
1.000×10^3	spline3	4.230×10^{-1}	2.279×10^{-2}	1.795×10^{-1}	
1.000×10^3	rf	1.072×10^{-1}	3.980×10^{-2}	1.308×10^{-2}	49%
1.000×10^3	BART	3.278×10^{-1}	5.504×10^{-2}	1.105×10^{-1}	0%
1.000×10^3	DML_gp3	3.572×10^{-1}	2.244×10^{-2}	1.281×10^{-1}	
1.000×10^3	DML_spline	3.324×10^{-1}	2.567×10^{-2}	1.111×10^{-1}	
1.000×10^3	DML_BART	3.204×10^{-1}	5.549×10^{-2}	1.057×10^{-1}	0%
1.000×10^4	RSR	4.197×10^{-1}	1.015×10^{-2}	1.763×10^{-1}	0%
1.000×10^4	spline	2.879×10^{-1}	7.850×10^{-3}	8.295×10^{-2}	0%
1.000×10^4	gp	2.880×10^{-1}	7.820×10^{-3}	8.299×10^{-2}	0%
1.000×10^4	gSEM	3.007×10^{-1}	8.043×10^{-3}	9.051×10^{-2}	0%
1.000×10^4	spatial+	2.879×10^{-1}	7.798×10^{-3}	8.296×10^{-2}	0%
1.000×10^4	spline_interaction	3.443×10^{-1}	5.832×10^{-3}	1.186×10^{-1}	0%
1.000×10^4	spline3	3.678×10^{-1}	1.214×10^{-2}	1.354×10^{-1}	
1.000×10^4	rf	2.182×10^{-1}	1.239×10^{-2}	4.775×10^{-2}	0%
1.000×10^4	BART	3.194×10^{-1}	2.167×10^{-2}	1.025×10^{-1}	0%
1.000×10^4	DML_spline	3.373×10^{-1}	1.202×10^{-2}	1.139×10^{-1}	
1.000×10^4	DML_BART	3.255×10^{-1}	2.052×10^{-2}	1.064×10^{-1}	0%

Table 5: Noisy confounding simulation results

6.3.7 Smooth exposure

$$S^a, S^b \sim_{iid} \text{unif}(-1, 1)$$

$$U = \sin(2\pi S^a * S^b) + S^a + S^b$$

$$X = C^3 + \cos(2\pi S^a * S^b)$$

$$Y \sim N(3C + X, 1)$$

When the exposure is a perfectly smooth function of spatial location, 7, just as the unmeasured confounder is, their effects cannot be disentangled by any of the models; this can be seen as an extreme violation of positivity. Because of this, all models exhibit substantial error. (Some of the spline-based methods exhibit decent confidence interval coverage, presumably due to computational instability in the bootstrap distribution arising from the concurvity.)

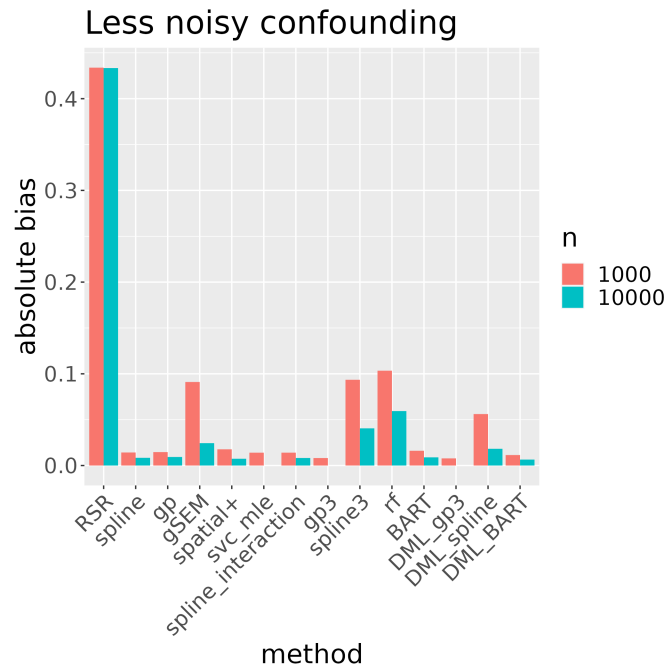


Figure 6: Absolute bias in the less noisy confounding scenario

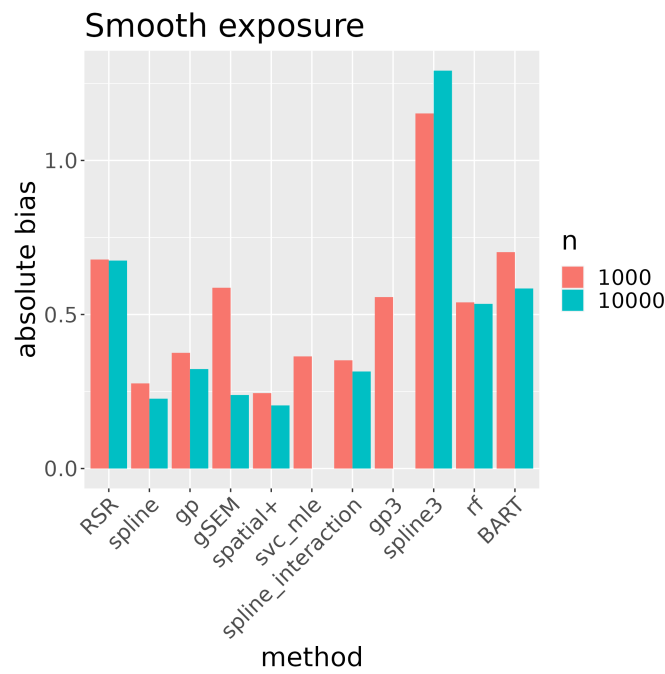


Figure 7: Absolute bias in the smooth exposure scenario

n	method	bias	sd	mse	coverage
1.000×10^3	RSR	4.338×10^{-1}	2.410×10^{-2}	1.888×10^{-1}	0%
1.000×10^3	spline	1.421×10^{-2}	7.492×10^{-3}	2.581×10^{-4}	49%
1.000×10^3	gp	1.464×10^{-2}	7.791×10^{-3}	2.748×10^{-4}	49%
1.000×10^3	gSEM	9.108×10^{-2}	9.040×10^{-3}	8.378×10^{-3}	0%
1.000×10^3	spatial+	1.768×10^{-2}	7.902×10^{-3}	3.750×10^{-4}	45%
1.000×10^3	svc_mle	1.401×10^{-2}	7.693×10^{-3}	2.553×10^{-4}	
1.000×10^3	spline_interaction	1.403×10^{-2}	7.515×10^{-3}	2.532×10^{-4}	81%
1.000×10^3	gp3	8.156×10^{-3}	7.658×10^{-3}	1.251×10^{-4}	
1.000×10^3	spline3	9.351×10^{-2}	6.410×10^{-2}	1.284×10^{-2}	
1.000×10^3	rf	-1.034×10^{-1}	2.001×10^{-2}	1.109×10^{-2}	2%
1.000×10^3	BART	1.608×10^{-2}	1.896×10^{-2}	6.173×10^{-4}	100%
1.000×10^3	DML_gp3	7.789×10^{-3}	7.932×10^{-3}	1.235×10^{-4}	
1.000×10^3	DML_spline	5.611×10^{-2}	5.497×10^{-2}	6.164×10^{-3}	
1.000×10^3	DML_BART	1.143×10^{-2}	1.889×10^{-2}	4.865×10^{-4}	100%
1.000×10^4	RSR	4.334×10^{-1}	7.335×10^{-3}	1.879×10^{-1}	0%
1.000×10^4	spline	8.398×10^{-3}	2.300×10^{-3}	7.579×10^{-5}	6%
1.000×10^4	gp	9.312×10^{-3}	2.298×10^{-3}	9.197×10^{-5}	2%
1.000×10^4	gSEM	2.439×10^{-2}	2.461×10^{-3}	6.009×10^{-4}	0%
1.000×10^4	spatial+	7.380×10^{-3}	2.299×10^{-3}	5.973×10^{-5}	11%
1.000×10^4	spline_interaction	8.209×10^{-3}	2.306×10^{-3}	7.269×10^{-5}	7%
1.000×10^4	spline3	4.054×10^{-2}	1.026×10^{-2}	1.748×10^{-3}	
1.000×10^4	rf	-5.936×10^{-2}	5.370×10^{-3}	3.553×10^{-3}	0%
1.000×10^4	BART	8.915×10^{-3}	3.818×10^{-3}	9.399×10^{-5}	64%
1.000×10^4	DML_spline	1.824×10^{-2}	1.001×10^{-2}	4.325×10^{-4}	
1.000×10^4	DML_BART	6.480×10^{-3}	3.778×10^{-3}	5.621×10^{-5}	84%

Table 6: Less noisy confounding simulation results

Summary of simulations These simulations confirm multiple strands of argument from the body of the paper. First, effect heterogeneity and nonlinearity can result in severe bias in models which are unable to account for them. On the other hand, with the noted exception of random forest, flexible models perform well, even competitive with simpler models when the simpler models are correctly specified. DML methods tend to reduce bias and MSE compared to their (single) machine learning counterparts. The assumptions of smooth confounding through space and extra-spatial variation in the exposure of interest have proven to be critical, though small departures from smoothness of the confounding surface were not severely harmful.

n	method	bias	sd	mse	coverage
1.000×10^3	RSR	6.784×10^{-1}	3.030×10^{-2}	4.611×10^{-1}	0%
1.000×10^3	spline	2.763×10^{-1}	2.757×10^{-2}	7.712×10^{-2}	0%
1.000×10^3	gp	3.755×10^{-1}	2.176×10^{-2}	1.415×10^{-1}	0%
1.000×10^3	gSEM	5.868×10^{-1}	3.014×10^{-1}	4.350×10^{-1}	73%
1.000×10^3	spatial+	2.448×10^{-1}	3.007×10^{-1}	1.502×10^{-1}	94%
1.000×10^3	svc_mle	3.640×10^{-1}	4.203×10^{-2}	1.342×10^{-1}	
1.000×10^3	spline_interaction	3.513×10^{-1}	6.681×10^{-2}	1.279×10^{-1}	99%
1.000×10^3	gp3	5.565×10^{-1}	8.876×10^{-2}	3.175×10^{-1}	
1.000×10^3	spline3	1.153×10^0	1.582×10^{-1}	1.353×10^0	
1.000×10^3	rf	5.394×10^{-1}	8.793×10^{-2}	2.986×10^{-1}	0%
1.000×10^3	BART	7.024×10^{-1}	1.265×10^{-1}	5.093×10^{-1}	1%
1.000×10^4	RSR	6.750×10^{-1}	9.106×10^{-3}	4.557×10^{-1}	0%
1.000×10^4	spline	2.267×10^{-1}	1.188×10^{-2}	5.152×10^{-2}	0%
1.000×10^4	gp	3.229×10^{-1}	7.812×10^{-3}	1.043×10^{-1}	0%
1.000×10^4	gSEM	2.386×10^{-1}	7.345×10^{-2}	6.231×10^{-2}	10%
1.000×10^4	spatial+	2.049×10^{-1}	7.285×10^{-2}	4.726×10^{-2}	20%
1.000×10^4	spline_interaction	3.150×10^{-1}	4.915×10^{-2}	1.016×10^{-1}	98%
1.000×10^4	spline3	1.292×10^0	9.115×10^{-2}	1.676×10^0	
1.000×10^4	rf	5.344×10^{-1}	3.208×10^{-2}	2.867×10^{-1}	0%
1.000×10^4	BART	5.844×10^{-1}	6.789×10^{-2}	3.461×10^{-1}	0%

Table 7: Smooth exposure simulation results

7 Discussion

In this paper, we have argued that spatial confounding can be understood most clearly as omitted variable bias. We have given conditions sufficient for the identification and estimation of causal effects when unmeasured confounders are associated with spatial location. The two most basic requirements for estimation is that, the exposure of interest should not be perfectly spatially smooth, and there should not be random (nonspatial) variation in the unmeasured confounder. We recommend the use of flexible models to estimate causal effects rather than the restrictive linear models that are typically used in spatial statistics; the assumptions of linearity and homogeneity are often implausible in practice and can lead to high bias. In addition, DML methods, widely known among causal inference researchers, should be considered strong candidates for spatial models.

There remains much room for further research. For example, unmeasured confounders will often be associated with spatial location even if they are not smooth functions of spatial location. In this scenario, it would be beneficial to quantify the extent to which omitted variable bias can be reduced by including spatial location in the causal model and/or provide a framework for sensitivity analysis for causal estimates. The assessment of exposures that are smooth in space (for example, distance to some location such as a factory) is beyond the reach of our current methods, but may be possible under certain assumptions about relevant scales of variation, as in Paciorek (2010) and Keller and Szpiro (2020). In addition, the mitigation of spatial confounding for areal data has been mostly ignored in this work as some fundamental concepts are distinct in the areal domain; with discrete locations, it is not possible for a confounding variable to be a smooth function, and it is not obvious how to consider an asymptotic regime as the number of areal units are is typically fixed.

References

- Joshua Angrist. Treatment effect heterogeneity in theory and practice. Working Paper 9708, National Bureau of Economic Research, 2003. URL https://www.nber.org/system/files/working_papers/w9708/w9708.pdf.
- Sudipto Banerjee, Alan E. Gelfand, Andrew O. Finley, and Huiyan Sang. Gaussian predictive process models for large spatial data sets. *Journal of the Royal Statistical Society. Series B (Statistical Methodology)*, 70(4):825–848, September 2008. doi: 10.1111/j.1467-9868.2008.00663.x. URL <https://doi.org/10.1111/j.1467-9868.2008.00663.x>.
- D Benkeser, M Carone, M J Van Der Laan, and P B Gilbert. Doubly robust nonparametric inference on the average treatment effect. *Biometrika*, 104(4):863–880, October 2017. doi: 10.1093/biomet/asx053. URL <https://doi.org/10.1093/biomet/asx053>.
- Julian Besag. Spatial interaction and the statistical analysis of lattice systems. *Journal of the Royal Statistical Society. Series B (Methodological)*, 36(2):192–236, 1974. ISSN 00359246. URL <http://www.jstor.org/stable/2984812>.
- Leo Breiman. Random forests. *Machine Learning*, 45(1):5–32, 2001. doi: 10.1023/a:1010933404324. URL <https://doi.org/10.1023/a:1010933404324>.
- Victor Chernozhukov, Denis Chetverikov, Mert Demirer, Esther Duflo, Christian Hansen, Whitney Newey, and James Robins. Double/debiased machine learning for treatment and structural parameters. *The Econometrics Journal*, 21(1):C1–C68, January 2018. ISSN 1368-4221. doi: 10.1111/ectj.12097. URL <https://doi.org/10.1111/ectj.12097>.
- Hugh A. Chipman, Edward I. George, and Robert E. McCulloch. BART: Bayesian additive regression trees. *The Annals of Applied Statistics*, 4(1):266 – 298, 2010. doi: 10.1214/09-AOAS285. URL <https://doi.org/10.1214/09-AOAS285>.
- Christopher Cox. Threshold dose-response models in toxicology. *Biometrics*, 43(3):511–523, 1987. ISSN 0006341X, 15410420. URL <http://www.jstor.org/stable/2531991>.
- Noel A. C. Cressie. *Statistics for Spatial Data*. John Wiley & Sons, Inc., September 1993. doi: 10.1002/9781119115151. URL <https://doi.org/10.1002/9781119115151>.

- Jakob A. Dambon, Fabio Sigrist, and Reinhard Furrer. Maximum likelihood estimation of spatially varying coefficient models for large data with an application to real estate price prediction. *Spatial Statistics*, 41:100470, March 2021a. doi: 10.1016/j.spasta.2020.100470. URL <https://doi.org/10.1016/j.spasta.2020.100470>.
- Jakob A. Dambon, Fabio Sigrist, and Reinhard Furrer. *varycoef: Modeling Spatially Varying Coefficients*, 2021b. URL <https://CRAN.R-project.org/package=varycoef>.
- Alexander D’Amour, Peng Ding, Avi Feller, Lihua Lei, and Jasjeet Sekhon. Overlap in observational studies with high-dimensional covariates. *Journal of Econometrics*, 221(2):644–654, April 2021. doi: 10.1016/j.jeconom.2019.10.014. URL <https://doi.org/10.1016/j.jeconom.2019.10.014>.
- Francesca Dominici, Michael Daniels, Scott L Zeger, and Jonathan M Samet. Air pollution and mortality. *Journal of the American Statistical Association*, 97(457):100–111, March 2002. doi: 10.1198/016214502753479266. URL <https://doi.org/10.1198/016214502753479266>.
- Francesca Dominici, Aidan McDermott, and Trevor J Hastie. Improved semiparametric time series models of air pollution and mortality. *Journal of the American Statistical Association*, 99(468):938–948, 2004. doi: 10.1198/016214504000000656. URL <https://doi.org/10.1198/016214504000000656>.
- Vincent Dorie. dbarts: Discrete bayesian additive regression trees sampler, 2020. URL <https://CRAN.R-project.org/package=dbarts>. R package version 0.9-19.
- Olivier Dubrule. Comparing splines and kriging. *Computers & Geosciences*, 10(2):327–338, 1984. ISSN 0098-3004. doi: 10.1016/0098-3004(84)90030-X. URL <https://www.sciencedirect.com/science/article/pii/009830048490030X>.
- Emiko Dupont, Simon N. Wood, and Nicole Augustin. Spatial+: a novel approach to spatial confounding. arXiv 2009.09420, 2020.
- Bradley Efron. Better bootstrap confidence intervals. *Journal of the American Statistical Association*, 82(397):171–185, March 1987. doi: 10.1080/01621459.1987.10478410. URL <https://doi.org/10.1080/01621459.1987.10478410>.

- Felix Elwert and Christopher Winship. Endogenous selection bias: The problem of conditioning on a collider variable. *Annual Review of Sociology*, 40(1):31–53, July 2014. doi: 10.1146/annurev-soc-071913-043455. URL <https://doi.org/10.1146/annurev-soc-071913-043455>.
- Jianqing Fan and Tao Huang. Profile likelihood inferences on semiparametric varying-coefficient partially linear models. *Bernoulli*, 11(6), December 2005. doi: 10.3150/bj/1137421639. URL <https://doi.org/10.3150/bj/1137421639>.
- Montserrat Fuentes. Approximate likelihood for large irregularly spaced spatial data. *Journal of the American Statistical Association*, 102(477):321–331, March 2007. doi: 10.1198/016214506000000852. URL <https://doi.org/10.1198/016214506000000852>.
- Dani Gamerman, Ajax R.B. Moreira, and Håvard Rue. Space-varying regression models: specifications and simulation. *Computational Statistics & Data Analysis*, 42(3):513–533, March 2003. doi: 10.1016/S0167-9473(02)00211-6. URL [https://doi.org/10.1016/S0167-9473\(02\)00211-6](https://doi.org/10.1016/S0167-9473(02)00211-6).
- Alan E Gelfand, Hyon-Jung Kim, CF Sirmans, and Sudipto Banerjee. Spatial modeling with spatially varying coefficient processes. *Journal of the American Statistical Association*, 98(462):387–396, 2003.
- N. Gouveia. Time series analysis of air pollution and mortality: effects by cause, age and socioeconomic status. *Journal of Epidemiology & Community Health*, 54(10):750–755, October 2000. doi: 10.1136/jech.54.10.750. URL <https://doi.org/10.1136/jech.54.10.750>.
- Mengyang Gu, Jesus Palomo, and James Berger. *RobustGaSP: Robust Gaussian Stochastic Process Emulation*, 2020. URL <https://CRAN.R-project.org/package=RobustGaSP>. R package version 0.6.1.
- Yawen Guan, Garritt L. Page, Brian J Reich, Massimo Ventrucchi, and Shu Yang. A spectral adjustment for spatial confounding, 2020.
- S. Haneuse and A. Rotnitzky. Estimation of the effect of interventions that modify the received treatment. *Statistics in Medicine*, 32(30):5260–5277, 2013. doi: <https://doi.org/10.1002/sim.5907>. URL <https://onlinelibrary.wiley.com/doi/abs/10.1002/sim.5907>.

- Sebastien Haneuse, Tyler J. VanderWeele, and David Arterburn. Using the e-value to assess the potential effect of unmeasured confounding in observational studies. *JAMA*, 321(6):602, February 2019. doi: 10.1001/jama.2018.21554. URL <https://doi.org/10.1001/jama.2018.21554>.
- James S. Hodges and Brian J. Reich. Adding spatially-correlated errors can mess up the fixed effect you love. *The American Statistician*, 64(4):325–334, 2010. doi: 10.1198/tast.2010.10052. URL <https://doi.org/10.1198/tast.2010.10052>.
- Joshua P. Keller and Adam A. Szpiro. Selecting a scale for spatial confounding adjustment. *Journal of the Royal Statistical Society: Series A (Statistics in Society)*, 183(3):1121–1143, 2020. doi: <https://doi.org/10.1111/rssa.12556>. URL <https://rss.onlinelibrary.wiley.com/doi/abs/10.1111/rssa.12556>.
- E. H. Kennedy, Z. Ma, M. D. McHugh, and D. S. Small. Nonparametric methods for doubly robust estimation of continuous treatment effects. *Journal of the Royal Statistical Society: Series B (Statistical Methodology)*, 79(4):1229–1245, Sep 2017.
- Edward H. Kennedy. Nonparametric causal effects based on incremental propensity score interventions. *Journal of the American Statistical Association*, 114(526):645–656, 2019. doi: 10.1080/01621459.2017.1422737. URL <https://doi.org/10.1080/01621459.2017.1422737>.
- Kori Khan and Catherine A. Calder. Restricted spatial regression methods: Implications for inference. *Journal of the American Statistical Association*, 0(0):1–13, 2020. doi: 10.1080/01621459.2020.1788949. URL <https://doi.org/10.1080/01621459.2020.1788949>.
- Manabu Kuroki and Judea Pearl. Measurement bias and effect restoration in causal inference. *Biometrika*, 101(2):423–437, 2014.
- Timothy L Lash, Tyler J VanderWeele, and Kenneth J Rothman. Measurement and measurement error. *Modern Epidemiology*, 2020.
- Lihua Lei and Emmanuel J. Candès. Conformal inference of counterfactuals and individual treatment effects, 2021.
- Andy Liaw and Matthew Wiener. Classification and regression by randomforest. *R News*, 2(3): 18–22, 2002. URL <https://CRAN.R-project.org/doc/Rnews/>.

- Ashley I Naimi, Alan E Mishler, and Edward H Kennedy. Challenges in obtaining valid causal effect estimates with machine learning algorithms, 2020.
- Elizabeth L Ogburn and Tyler J VanderWeele. On the nondifferential misclassification of a binary confounder. *Epidemiology (Cambridge, Mass.)*, 23(3):433, 2012.
- Elizabeth L Ogburn and Tyler J Vanderweele. Bias attenuation results for nondifferentially mismeasured ordinal and coarsened confounders. *Biometrika*, 100(1):241–248, 2013.
- Muhammad Osama, Dave Zachariah, and Thomas B. Schön. Inferring heterogeneous causal effects in presence of spatial confounding. In Kamalika Chaudhuri and Ruslan Salakhutdinov, editors, *Proceedings of the 36th International Conference on Machine Learning*, volume 97 of *Proceedings of Machine Learning Research*, pages 4942–4950. PMLR, June 2019. URL <http://proceedings.mlr.press/v97/osama19a.html>.
- Christopher J. Paciorek. The Importance of Scale for Spatial-Confounding Bias and Precision of Spatial Regression Estimators. *Statistical Science*, 25(1):107 – 125, 2010. doi: 10.1214/10-STS326. URL <https://doi.org/10.1214/10-STS326>.
- Georgia Papadogeorgou, Christine Choirat, and Corwin M Zigler. Adjusting for unmeasured spatial confounding with distance adjusted propensity score matching. *Biostatistics*, 20(2): 256–272, January 2018. ISSN 1465-4644. doi: 10.1093/biostatistics/kxx074. URL <https://doi.org/10.1093/biostatistics/kxx074>.
- Jose M Peña, Sourabh Balgi, Arvid Sjölander, and Erin E Gabriel. On the bias of adjusting for a non-differentially mismeasured discrete confounder. *Journal of Causal Inference*, 9(1):229–249, 2021.
- M. L. Petersen, K. E. Porter, S. Gruber, Y. Wang, and M. J. van der Laan. Diagnosing and responding to violations in the positivity assumption. *Statistical Methods in Medical Research*, 21(1):31–54, Feb 2012.
- C. C. Pugh. *Real mathematical analysis*. Springer, Cham, 2015. ISBN 978-3-319-17771-7.
- Timothy Ramsay, Richard Burnett, and Daniel Krewski. Exploring bias in a generalized additive model for spatial air pollution data. *Environmental Health Perspectives*, 111(10):1283–1288, August 2003. doi: 10.1289/ehp.6047. URL <https://doi.org/10.1289/ehp.6047>.

- John Rice. Convergence rates for partially splined models. *Statistics & Probability Letters*, 4(4): 203–208, 1986. ISSN 0167-7152. doi: [https://doi.org/10.1016/0167-7152\(86\)90067-2](https://doi.org/10.1016/0167-7152(86)90067-2). URL <https://www.sciencedirect.com/science/article/pii/0167715286900672>.
- Donald B. Rubin. Estimating causal effects of treatments in randomized and nonrandomized studies. *Journal of Educational Psychology*, 66(5):688–701, 1974. doi: 10.1037/h0037350. URL <https://doi.org/10.1037/h0037350>.
- Arkajyoti Saha and Abhirup Datta. Brisc: bootstrap for rapid inference on spatial covariances. *Stat*, 7(1):e184, 2018. doi: <https://doi.org/10.1002/sta4.184>. URL <https://onlinelibrary.wiley.com/doi/abs/10.1002/sta4.184>. e184 sta4.184.
- Arkajyoti Saha and Abhirup Datta. *BRISC: Fast Inference for Large Spatial Datasets using BRISC*, 2020. URL <https://CRAN.R-project.org/package=BRISC>. R package version 0.3.0.
- Arkajyoti Saha, Sumanta Basu, and Abhirup Datta. Random forests for spatially dependent data. *Journal of the American Statistical Association*, pages 1–19, 2021.
- Patrick M. Schnell and Georgia Papadogeorgou. Mitigating unobserved spatial confounding when estimating the effect of supermarket access on cardiovascular disease deaths. *The Annals of Applied Statistics*, 14(4):2069 – 2095, 2020. doi: 10.1214/20-AOAS1377. URL <https://doi.org/10.1214/20-AOAS1377>.
- Fabio Sigrist. Gaussian process boosting. *arXiv preprint arXiv:2004.02653*, 2020.
- Michael L. Stein. Limitations on low rank approximations for covariance matrices of spatial data. *Spatial Statistics*, 8:1–19, May 2014. doi: 10.1016/j.spasta.2013.06.003. URL <https://doi.org/10.1016/j.spasta.2013.06.003>.
- Elizabeth A. Stuart. Matching methods for causal inference: A review and a look forward. *Statistical Science*, 25(1), February 2010. doi: 10.1214/09-sts313. URL <https://doi.org/10.1214/09-sts313>.
- Eric J Tchetgen Tchetgen, Andrew Ying, Yifan Cui, Xu Shi, and Wang Miao. An introduction to proximal causal learning. *arXiv preprint arXiv:2009.10982*, 2020.

- Hauke Thaden and Thomas Kneib. Structural equation models for dealing with spatial confounding. *The American Statistician*, 72(3):239–252, 2018. doi: 10.1080/00031305.2017.1305290. URL <https://doi.org/10.1080/00031305.2017.1305290>.
- W. R. Tobler. A computer movie simulating urban growth in the detroit region. *Economic Geography*, 46:234–240, 1970. ISSN 00130095, 19448287. URL <http://www.jstor.org/stable/143141>.
- T. J. VanderWeele and I. Shpitser. On the definition of a confounder. *The Annals of Statistics*, 41(1):196–220, Feb 2013.
- Stefan Wager and Susan Athey. Estimation and inference of heterogeneous treatment effects using random forests. *Journal of the American Statistical Association*, 113(523):1228–1242, June 2018. doi: 10.1080/01621459.2017.1319839. URL <https://doi.org/10.1080/01621459.2017.1319839>.
- Daniel Westreich and Stephen R. Cole. Invited Commentary: Positivity in Practice. *American Journal of Epidemiology*, 171(6):674–677, February 2010. ISSN 0002-9262. doi: 10.1093/aje/kwp436. URL <https://doi.org/10.1093/aje/kwp436>.
- Christopher K. Wikle and Mevin B. Hooten. A general science-based framework for dynamical spatio-temporal models. *TEST*, 19(3):417–451, November 2010. doi: 10.1007/s11749-010-0209-z. URL <https://doi.org/10.1007/s11749-010-0209-z>.
- Simon Wood. *mgcv: Mixed GAM Computation Vehicle with Automatic Smoothness Estimation*, 2003a. URL <https://cran.r-project.org/web/packages/mgcv/index.html>.
- Simon N. Wood. Thin plate regression splines. *Journal of the Royal Statistical Society: Series B (Statistical Methodology)*, 65(1):95–114, 2003b. doi: <https://doi.org/10.1111/1467-9868.00374>. URL <https://rss.onlinelibrary.wiley.com/doi/abs/10.1111/1467-9868.00374>.
- Yun Yang, Guang Cheng, and David B. Dunson. Semiparametric bernstein-von mises theorem: Second order studies, 2015.
- Dale L. Zimmerman and Jay M. Ver Hoef. On deconfounding spatial confounding in linear models. *The American Statistician*, 0(0):1–9, 2021. doi: 10.1080/00031305.2021.1946149. URL <https://doi.org/10.1080/00031305.2021.1946149>.